Hepatitis C virus is released via a non-canonical secretory route.

Karen Bayer[1], Carina Banning[3], Volker Bruss[1], Linda Wiltzer-Bach[2], and Michael Schindler[1,2,3,*]

[1]Institute of Virology, Helmholtz Zentrum München - German Research Center for Environmental Health, Munich, Germany

[2]University Hospital Tübingen, Institute for Medical Virology and Epidemiology of Viral Diseases, Tübingen, Germany

[3]Heinrich Pette Institute, Leibniz Institute for Experimental Virology, Hamburg, Germany

[*]*Address correspondence to:*
Michael Schindler
University Hospital Tübingen, Institute for Medical Virology
Elfriede-Aulhorn-Str. 6
72076 Tübingen, Germany
Phone: +49-7071-2987469
FAX: +49-7071-295419
michael.schindler@med.uni-tuebingen.de

Short title: Non-canonical release of HCV.

Keywords: Hepatitis C virus, morphogenesis, release, live cell imaging, trafficking

ABSTRACT

We analyzed HCV morphogenesis using viral genomes encoding for a mCherry-tagged E1 glycoprotein. HCV-E1-mCherry polyprotein expression, intracellular localization and replication kinetics were comparable to untagged HCV and E1-mCherry tagged viral particles were assembled and released into cell culture supernatants. Expression and localization of structural E1 and non-structural NS5A followed a tempo-spatial pattern with succinct decrease in replication complexes and the appearance of E1-mCherry punctae. Interaction of the structural proteins E1, Core and E2 increased at E1-mCherry punctae in a time-dependent manner, indicating that E1-mCherry punctae represent assembled or assembling virions. E1-mCherry did not colocalize with Golgi markers. Furthermore, the bulk of viral glycoproteins within released particles revealed an EndoH-sensitive glycosylation pattern, indicating absence of viral glycoprotein processing by the Golgi. In contrast, HCV-E1-mCherry trafficked with Rab9-positive compartments and inhibition of endosomes specifically suppressed HCV release. Our data suggests that assembled HCV particles are released via a non-canonical secretory route involving the endosomal compartment.

47

48 **IMPORTANCE STATEMENT**

49 The goal of this study was to shed light on the poorly understood trafficking and release routes of
50 hepatitis C virus (HCV). For this, we generated novel HCV genomes which result in the
51 production of fluorescently labeled viral particles. We used live cell microscopy and other
52 imaging techniques to follow up on the temporal dynamics of virus particle formation and
53 trafficking in HCV-expressing liver cells. While viral particles and viral structural protein were
54 found in endosomal compartments, no overlap with Golgi structures could be observed.
55 Furthermore, biochemical and inhibitor-based experiments support a HCV release route which is
56 distinguishable from canonical Golgi-mediated secretion. Since viruses hijack cellular pathways
57 to generate viral progeny, our results point towards the possible existence of a not yet described
58 cellular secretion route.

59

60

61 **INTRODUCTION**

62 Hepatitis C virus (HCV) belongs to the flavivirus genus and has a positive-strand RNA genome.
63 This encodes a polyprotein which is post-translationally cleaved into six non-structural (NS)
64 proteins, the ion-channel p7 and the structural proteins Core, E1 and E2 (1). The NS proteins
65 reside at the outer leaflet of the endoplasmic reticulum (ER) membrane where particularly NS4B
66 and NS5A induce membrane alterations resulting in the formation of the membranous web,
67 which is the major site for HCV replication (2-5). Core is targeted to adjacent lipid droplets (LD)
68 (6, 7), which represent intracellular lipid deposits and are considered important for production of
69 infectious particles (1, 7, 8). The envelope proteins E1 and E2 are incorporated into ER
70 membranes with ectodomains facing the ER lumen (9, 10). Later, they are recruited to assembly
71 sites via the NS2 complex (11, 12). Upon recruitment of all required viral components, HCV
72 assembly is thought to occur at the surface of LDs (6-8, 13).
73 The mechanisms that trigger switching from polyprotein translation to viral RNA replication and
74 then to the initiation of virus assembly are largely unknown. Recently, it has been proposed that
75 the cellular Ewing sarcoma breakpoint region 1 (EWSR1) protein is important to regulate the
76 switch from translation to replication by binding to the *cis*-acting replication element of HCV
77 (14). Furthermore, transport of HCV Core towards LDs by the enzyme diacylglycerol
78 acyltransferase-1 (DGAT1) is crucial for production of newly formed virions (15, 16) and the
79 NS2 protein together with p7 might be major players in coordinating assembly (17-19).
80 How HCV is released from infected cells is still under debate. HCV was found to associate with
81 constituents of very low density lipoproteins (VLDL), such as ApoB and ApoE (20-22), and
82 proteins of the VLDL secretory pathway including the transcription factor Hepatocyte Nuclear
83 Factor 4 (HNF4) (23). Thus, it has been assumed that HCV budding, maturation and release

might intersect the VLDL secretion pathway (24), but a precise model is still lacking and a recent study suggests that HCV release is independent of the VLDL route (25).

Other members of the Flaviviridae, e.g. dengue virus or bovine viral diarrhoea virus, are released through classical secretion via the Golgi apparatus and the *trans*-Golgi network (26-28). Therefore a similar mechanism has been postulated for HCV. In a recent study the PI4P-binding protein GOLPH3 was suggested to have a role in HCV budding since silencing of this protein lead to reduced levels of HCV release (29). Similarly, a siRNA screen that targeted 140 cellular membrane trafficking genes has identified components of the classical secretion pathway that affected the release of HCV (30). However, silencing such cellular membrane trafficking genes might have effects on the processing of proteins that are involved in other, possibly yet unknown, intracellular trafficking and secretion pathways, which could be essential to the release of HCV (31). Furthermore, such interventions are very likely to influence various cellular processes and signaling pathways. As an example, GOLPH3 is also a key player in modulation of mTOR signaling (32).

In order to investigate the process of HCV assembly, budding and release we constructed HCV genomes with a fluorescent tag within the E1 protein (Jc1-E1(A4)-mCherry). We also inserted this tag in combination with a previously described GFP-tagged NS5A genome (33) generating the Jc1-E1(A4)-mCherry/NS5A-GFP virus, which allows simultaneous visualization of structural protein expression and replication complexes. Live cell observations and confocal microscopy of HCV-expressing Huh7.5 cells revealed a distinct tempo-spatial organization of structural (E1) and non-structural (NS5A) protein expression. Detailed biochemical and microscopic analyses revealed the importance of the endosomal compartment for HCV egress and an unconventional secretory route hijacked by HCV for release.

107 **MATERIALS and METHODS**

108 **HCV constructs and expression plasmids.** The following HCV constructs were kind gifts from
109 R. Bartenschlager, (University of Heidelberg): pFK_Jc1 (34), pFK_Jc1-luc (34), pFK_Jc1-Flag-
110 E2 (35) and pFK_Jc1-NS5A-GFP (33). To generate HCV with a fluorescently labeled structural
111 protein (pFK_Jc1-E1-mCherry) we amplified mCherry (primers: 5'mCherry-*BsiWI* 5'-
112 ggcgtacgcgatggtgagcaagggcgag-3'; 3'mCherry-*BsiWI* 5'-cgcgtacgccttgtacagctcgtccatgcc-3') and
113 introduced flanking *BsiWI* restriction sites, then ligated mCherry into the *BsiWI* site present
114 between the last glycosylation site and the transmembrane domain of E1 in pFK_Jc1. The
115 nucleotide sequence was confirmed by Sanger sequencing. The double-labeled HCV genome
116 expressing E1-mCherry and NS5A-GFP (pFK_Jc1-E1-mCherry/NS5A-GFP) was generated by
117 the same cloning strategy, but mCherry was inserted into pFK_Jc1-NS5A-GFP. The variants
118 with the reconstituted HCV H77 E1-A4 epitope sequence (36) were generated by initial
119 reconstitution of the A4 epitope in the pFK_Jc1 by site directed mutagenesis. Then the other
120 variants were cloned as described above. A YFP-fusion construct of the secreted Gaussia
121 luciferase (37) was constructed by PCR amplification (primers: 5'Gaussia *NheI* 5'-
122 CCGGCTAGCatgggagtcaaagttctgtttg-3' and 3'Gaussia *AgeI* 5'-
123 TCGACCGGTGCACCTGCTCCgtcaccaccggccccttgatc-3') and ligation into the Clontech
124 vector pEYFP-N1 as described before (38). Similarly, we constructed the pECFP-CD74
125 expression vector. The mCherry-HBV-S construct was generated by fusing a sequence encoding
126 the secretion signal of beta-lactamase to the 5' end of the mCherry open reading frame and by
127 further fusion of this chimera to the 5'end of the HBV-S gene using standard PCR techniques.
128 Between the mCherry and HBV-S derived portions a linker sequence was inserted coding for the
129 peptide SLDPATSVDGGGGVDGGGGVEN. The CFP-GalT construct (39) was provided by P.

Bastiaens (MPI, Dortmund). pOPIN(n)eCFP-Rab7A and pOPIN(n)eCFP-Rab9A were gifts from A. Musacchio (MPI, Dortmund), GFP-VSVG from F. Perez (Institut Curie, Paris) and GFP-ApoE from G. Randall (University of Chicago).

Cell culture, transfection, HCV RNA electroporation. Huh7.5 cells (kindly provided by C. Rice, Rockefeller University) were cultured as previously described (40) and plasmids were coelectroporated with RNA of HCV Jc1 genomes using a BioRad Gene Pulser Xcell system. *In vitro* transcription of HCV RNA and electroporation were performed as previously described (41, 42). Briefly, the pFK plasmids were linearized by *MluI* digestion, purified with the Wizard® DNA Clean-Up system (Promega) and used for *in vitro* transcription with the help of the TranscriptAid T7 High Yield Transcription Kit (Fermentas). Both kits were used according to the manufacturer's instructions. The RNA was purified by phenol chloroform extraction and stored by - 80 °C. For electroporation $6x10^6$ cells and 5 µg RNA were used as previously described (42). Thereafter cells were seeded in well plates and media was changed after 6 hours.

Infectivity assay. 39 x 10^6 Huh7.5 cells were electroporated with RNA of each construct and seeded into two 175 cm^2 flasks. Supernatants of both flasks were pooled 65 hpe and cell debris was removed by centrifugation at 3000 rpm for 10 min before ultracentrifugation using a 20 % sucrose cushion at 28000 rpm for 90 min at 4°C. Pellets were resuspended in 400 µl medium at 4 °C over night. Naïve Huh7.5 cells were seeded in a 12-well plate (160,000 cells/well) and infected in a 400 µl volume for an incubation period of 6 h before cells were kept in fresh medium for 3 days. Then cells were trypsinized, washed in PBS and fixed in 2% PFA for 1 h at RT. Mock-infected cells were divided into two parts of which one was stained for intracellular Core together with cells infected with Jc1-E1(A4). For this, cells were treated with 1% saponin for 12 min at RT, washed twice in PBS and blocked in 10% goat serum for 20 min at RT before

153 they were incubated with primary antibody (mouse anti-Core, clone C7-50, Abcam) at a 1:100
154 dilution for 1 h at RT. The secondary antibody (goat anti-mouse Alexa633) was diluted 1:200 in
155 1% goat serum in PBS and cells were incubated for 1h at RT, washed twice in PBS and MFI was
156 analyzed using the BD FACS Canto-II or Aria-III.
157 **Virus purification and concentration.** Supernatant of vRNA electroporated cells was collected
158 72 hpe and cell debris was pelleted by centrifugation for 10 min at 3000 rpm. 32 ml of cleared
159 supernatant was transferred to an ultracentrifugation tube for the SW 28 rotor (Beckman
160 Coulter). Each supernatant was carefully underlaid with 5 ml 20% sucrose in PBS and
161 centrifuged using the Optima L7-65 Ultracentrifuge (Beckman Coulter) for 90 min at 28000 rpm
162 and 4 °C. Pelleted virus was dissolved in PBS or medium (50 to 100 µl) and resuspended for 16
163 h at 4°C.
164 **Fractionation of virus preparations.** Gradient fractions were prepared by mixing decreasing
165 amounts of serum free medium with increasing amounts of iodixanol density medium
166 (OptiPrep), to obtain fractions from 14, 18, 22, 26, 30, 34 and 38% iodixanol. Fractions were
167 transferred to an ultracentrifugation tube and subsequently overlaid with the concentrated virus
168 and centrifuged at 34000 rpm and 4 °C for 20 h in the Optima L7-65 Ultracentrifuge (Beckman
169 Coulter). The recovered fractions were diluted 1:2 with PBS and centrifuged again at 21000 x g
170 at 4°C for 90 min to concentrate virus particles or proteins in a pellet for downstream
171 applications.
172 **Endoglycosidase digestion.** 18 x 10^6 Huh7.5 cells were electroporated, cultured for 56 h in a
173 175 cm^2 flask, detached, washed and lysed with 0.5 % NP-40. In parallel, virus supernatant
174 collected from ten 175 cm^2 flasks was concentrated via ultracentrifugation or additional gradient
175 centrifugation and resuspended in 100 µl PBS each. 10 x Glycoprotein denaturation buffer

(NEB) was added to the supernatant after cell lysis or virus containing culture supernatant and boiled at 95°C for 10 min. Samples were subdivided into three equal parts: the untreated control, digested with EndoH (NEB) or with PNGaseF (NEB). Deglycosylation was done with the protocol provided by the manufacturer. Finally, 5 x SDS loading buffer was added to the samples and post boiling at 95°C they were further separated by SDS-PAGE and analyzed by Western blot.

Western blot. Two to three days post electroporation HCV producing Huh7.5 cells were pelleted, lysates were generated with standard RIPA buffer and proteins were separated through 12% SDS-PAGE. Expression of E2 and Core in whole cell lysates was analyzed by Western blot analysis using 1:500 diluted mouse anti-Core (clone C7-50; Abcam) or 1:100 diluted mouse anti-E2 AP33 antibody provided by Genentech (43). The anti-E1(A4) antibody was a kind gift from Harry Greenberg and used at 1:1000 dilution (36). The 1:5000 diluted mouse anti-β-actin (clone AC-15; Sigma-Aldrich) served as a loading control. mCherry was detected with a polyclonal rabbit antibody at 1:1000 dilution (BioVision) and the HBV-S protein with the mouse monoclonal HB1 antibody at 1:1000 dilution (kind gift from D. Glebe, Göttingen). For secondary antibody staining IRDye® 800 goat anti-mouse and IRDye® 680 goat anti-rabbit diluted 1:5000 (Li-Cor Biotechnology GmbH) or goat-anti mouse HRP and goat-anti rabbit HRP diluted 1:10000 (Dianova) were used. Detection was performed using either chemiluminescence or Odyssey infrared imaging system (LI-COR).

Coimmunoprecipitation. 18x10^6 Huh7.5 cells were electroporated with viral RNA detached 56 hpe and washed with cold PBS. Cells were sheared through a syringe in 800 µl CoIP lysis buffer (0.05 M Tris, 0.15 M NaCl, 1 mM EDTA, pH 7.4, 1 % Triton X-100 and fresh protease inhibitor) and rotated on a wheel for 20 min at 4°C before centrifugation of cell debris at 17000 g

for 10 min. The agarose-matrix coupled with anti-Flag tag antibodies (mouse anti-Flag; Sigma-Aldrich) was washed twice with CoIP wash buffer (0.05 M Tris, 0.15 M NaCl, pH 7.4) and once with 0.1 M glycin (pH 3.5) to remove unbound antibodies. After washing with CoIP wash buffer, the cleared protein containing supernatant as well as protease inhibitor (Roche) were added to 30 µl matrix and incubated on a wheel over night at 4 °C. Thereafter, the matrix was washed for removal of unspecific bound protein. Proteins were released from the matrix by 20 µl 5x SDS loading buffer (250 mM Tris-HCl (pH 6.8), 50% glycerol, 15% SDS, 0.01% bromophenol blue, 25% β-mercaptoethanol) and 5 min boiling at 95°C. Proteins in the precipitates were separated by SDS-PAGE and detected by Western blotting.

Flow cytometry and intracellular Core detection. Cells were detached with trypsin/EDTA, washed twice with PBS in FACS-tubes and were fixed for 20 min in 2% PFA and permeabilized for 10 min at RT in 1% saponin in PBS. Then washed twice and blocked with 10% goat serum in PBS for 30 min at RT. Cells were stained with primary antibody dilution (mouse anti-Core; Abcam) diluted 1:100 in 1 % goat serum in PBS for 1 h at 4 °C. After three washing steps cells were incubated with secondary antibody (Alexa Fluor® 633 goat anti-mouse, Life technologies) diluted 1:500 in 1 % goat serum in PBS at 4°C in the dark. After washing cells were analyzed using a BD FACS Canto-II or Aria-III.

Quantitative RT-PCR. For qRT-PCR measurement of viral RNA (vRNA) isolated by the NucleoSpin RNA Kit (Macherey Nagel) we used the OneStep RT-PCR Kit (Qiagen) that reversely transcribes and amplifies the RNA in the same reaction mix according to the manufacturer's instructions. We used the sample RNA and predefined standard dilution series of *in vitro* transcribed HCV-RNA and HCV-5' NCR specific primers (HCV fw 5'-gctagccgagtagcgttgggt-3' and HCV rev 5'-tgctcatggtgcacggtctacc-3') as well as the DNA probe

(5' FAM (Fluorescein)-tactgcctgatagggcgcttgcgagtg-TAMRA 3') for RT-PCR measurements with the LightCycler® 480 (Roche). The absolute quantification was performed with the help of a standard curve and the calculation of the absolute number of viral RNA copies within the samples.

Virus release and Gaussia secretion assay. To study virus release we used the Jc1-1uc reporter virus (34). As a control, the similar experiment was performed with cells expressing Gaussia luciferase. Huh7.5 cells were electroporated with viral RNA or a plasmid coding for a YFP-fused Gaussia luciferase construct. Cells were cultured for two days and medium was removed, cells were washed with PBS and inhibitor-containing medium was added. All inhibitors were dissolved in DMSO and used at the following concentrations which were found to be non-toxic on Huh7.5 cells by MTT test: 5 µg/ml Brefeldin A (AppliChem) and 25 µM U18666A (Cayman chemical). Eight hours post incubation virus containing supernatants were harvested and viral particles were purified to remove the inhibitors. A 20% sucrose-cushion was carefully overlaid with supernatant and centrifuged for 90 min at 20000 x *g* and 4 °C. The supernatant was withdrawn with a pipette without touching the pellet and the virus pellet was ressuspended in fresh medium. These cleared virus supernatants were used to inoculate Huh7.5 cells in a 96-well format. Three days later luciferase activity was assessed with the Luciferase Assay System (Promega) according to the manufacturer's instructions. Gaussia luciferase activity in the supernatant was measured directly with the BioLux Gaussia Luciferase Flex Assay Kit (NEB) as recommended by the manufacturer.

Biochemical fixation of the early endosomal compartment. The biochemical fixation of horseradish peroxidase (HRP) containing compartments has been described before (44, 45). We used that system to inactivate the early endosomal compartment as follows: two days post

electroporation HCV Jc1-luc or Gaussia luciferase expressing cells were starved for 90 min with medium containing 0.1 % FCS. Then cells were incubated for two hours at RT with medium containing 0.1 % FCS, 20 mM HEPES and 20 µg/ml Transferrin (Tf) as a control or HRP-coupled Transferrin (HRP-Tf), respectively. Cells were washed three times with cold PBS and incubated with 10 % FCS containing medium for ten minutes. Subsequently cells were kept on ice and diaminobenzidine (DAB) solution with 0.003 % H_2O_2 was added for 60min to inactivate the HRP-Tf containing endosomes. After washing with cold PBS complete medium was added and cells were allowed to produce virus or secrete Gaussia luciferase for further five hours. The amount of released virus or secreted Gaussia luciferase was assessed as described above.

Immunofluorescence and proximity ligation assay. HCV vRNA electroporated cells were grown in a 24-well plate on 12 mm cover slips and stained after the indicated time points. In brief, cells were washed and fixed for 20 min at 4 °C with 2 % PFA. Some samples were directly mounted using Mowiol 4-88 (Roth) or permeabilized for 10 min at RT with 1 % saponin and blocked with 10 % goat serum in PBS for 30 min at RT. Primary antibodies were diluted 1:100 in 1 % goat serum in PBS and incubated within a humid environment for 2 h at RT. Samples were washed to remove unbound antibodies and incubated with secondary antibodies (Alexa Fluor® 488, 555 or 633 goat anti-mouse; Life technologies) diluted 1:200 in 1 % goat serum/PBS for 1 h at RT in the dark. Post washing cover slips were mounted with Mowiol 4-88 (Roth), dried at RT for 16 h in the dark and analyzed by spinning disc confocal fluorescence microscopy (Nikon Ti Eclipse UltraViewVox System from Perkin Elmer). For PLA, cells were permeabilized and fixed as above, but blocking was done for 45 min with 5% BSA. Immunodetection was done with primary antibodies from rabbit directed against mCherry (BioVision) and either mouse anti E2 (AP-33), Core (C7-50, Abcam), NS3 (clone F3A6B2C3

against epitope 1322-1662 of JFH-1 NS3), or NS5A (2F6/G11, IBT) diluted 1:100 in 1 % BSA in PBS for 2 h at RT. Afterwards, samples were prepared according to the protocol of the manufacturer (Duolink, Sigma Aldrich) and as described (19). Spots of the fluorescent substrate were detected by confocal spinning disc microscopy (Nikon Ti Eclipse with the UltraViewVox System from Perkin Elmer). Quantitative analyses was performed using the Volocity software implemented automated spot counting tool with a defined maximum spot size of 0.8 µm.

Live cell imaging and fluorescence recovery after photobleaching (FRAP). Microscopy was performed with a fully motorized Nikon Ti-Eclipse inverted microscope equipped with the hardware based perfect focus system and the Perkin Elmer UltraViewVox Spinning Disc system. If not indicated otherwise, 0.45 x 10^6 Huh7.5 cells electroporated with RNA of the HCV Jc1 genomes were seeded in 35 mm dish with optical bottom (Ibidi or WillCo) and cultivated for the indicated times. Microscopy was performed in a humidified chamber with 5% CO_2 at 37 °C and a CFI Apochromat 60 X objective (NA 1.49) was used for imaging. Video sequences were processed using the Volocity software. For FRAP, electroporated Huh7.5 cells were seeded in a Willco-dish (WillCo) and cultured for 56 h. FRAP areas were selected by placing regions of interest and respective areas with background fluorescence. Time lapse imaging was started before bleach in 3 to 5 second intervals and continued for approximately 5 min later, depending on the experiment. Photobleaching was performed by a single pulse for 60000 ms. Intensity profiles of the different areas were computed with the Volocity software and Excel (Microsoft).

Image analysis and software. Microscopical sequences, colocalization analyses and spot counting was performed using the Volocity version 6.2 software package (Perkin Elmer). In general, images were never modified apart from enhancing contrast and/or brightness. Movies were generated and compressed with the freely available ImageJ (Fiji) and VirtualDub V1.10.4

291 software packages. Statistical analyses were performed using the GraphPad Prism 5.0 and 6.0
292 software package and two-tailed Student's t-test or multiple ANOVA tests.
293
294
295 **RESULTS**
296 **Construction and characterization of HCV genomes expressing fluorescently labeled**
297 **structural protein E1.**
298 To study HCV morphogenesis, the tempo-spatial dynamics of HCV structural protein expression
299 and the formation of replication complexes in living cells, we generated several HCV genomes
300 expressing fluorescently labeled E1 protein (Fig. 1A). The red monomeric fluorescent protein
301 mCherry (46) was inserted between the C-terminal glycosylation site of E1 and the stalk region
302 of the transmembrane domain (see materials and methods for details). We also reconstituted the
303 E1(A4) epitope from the strain HCV H77 enabling detection of E1 by a monoclonal antibody
304 (36). Using this strategy we generated HCV Jc1 (34) expressing an E1-mCherry fusion protein
305 (Jc1-E1(A4)-mCherry) as well as a variant co-expressing GFP within the NS5A protein (Jc1-
306 E1(A4)-mCherry/NS5A-GFP) (Figure 1A). Western blot analysis showed efficient expression of
307 the viral proteins Core, E1(A4)-mCherry, and E2 (Fig. 1B). Furthermore, the subcellular
308 localization of Core, NS5A, E2 and E1-mCherry in Huh7.5 cells electroporated with RNA of
309 Jc1-E1(A4)-mCherry was comparable to viral protein localization in cells electroporated with
310 RNA of Jc1-E1(A4) (Figure 1C).
311 Since insertion of mCherry into E1 might affect growth kinetics, we characterized the novel
312 HCV genomes in regards to viral replication and release of viral particles. First, we
313 electroporated Huh7.5 cells with RNA of the indicated HCV Jc1-E1(A4) variants, fixed and

314 stained for Core protein to assess the relative amount of HCV positive cells at different time
315 points over 64 hours post electroporation (hpe) using flow cytometry. All Jc1-E1(A4) variants
316 showed similar kinetics with the amount of Core-positive cells increasing until 40 hpe (Figure
317 2A). At later time points Core-positive cells of untagged Jc1-E1(A4) reached a plateau whereas
318 kinetics for all the variants expressing chromophore-tagged viral proteins slowly decreased. We
319 explain this by the strongly attenuated infectivity of the fluorescently labeled variants (Fig. 2B),
320 while the untagged Jc1 is capable of multiple rounds of reinfection and therefore spreading
321 within the cell culture.
322 Within the population of Core-expressing cells, the mean fluorescence intensity (MFI) of Core
323 protein staining was comparable between all variants indicating that the amount of viral protein
324 produced was similar (Fig. 2C). Also, the MFI of Core protein staining for all variants increased
325 over time, suggesting that within HCV-expressing cells protein production is not impaired. To
326 corroborate these results and to assess time dependent expression of other viral structural
327 proteins, we prepared cell lysates at the same time points for Western blot analysis. Similar to the
328 flow cytometry measurements, there was a clear increase in viral protein levels from 16 hpe to
329 48 hpe for Jc1-E1(A4) and Jc1-E1(A4)-mCherry/NS5A-GFP, not only for Core but also for the
330 viral glycoproteins E1 and E2 (Fig. 2D).
331 To analyze production of viral RNA (vRNA) over time we extracted total RNA from cells and
332 supernatants at 24, 40, 48 and 64 hpe and performed qRT-PCR. To calculate vRNA production
333 per HCV expressing cell we normalized the total amount of vRNA to the percentage of Core-
334 expressing cells, as measured by flow cytometry (comp. Fig. 2A). Intracellular vRNA levels
335 were initially high, reflecting the effective electroporation of RNA genomes, and increased
336 slightly with a plateau at 48 hpe (Fig. 2E). More importantly, extracellular vRNA levels,

337 reflecting released viral genomes, increased continuously over time indicating assembly and
338 release of viral particles for all of the tested variants (Fig. 2F). Notably, Jc1-E1(A4) RNA was
339 found to be approximately 10-fold increased in the supernatants compared to the fluorescently
340 labeled variants, which might reflect reduced packaging efficiency due to the increased size of
341 the chromophore encoding viral genomes. To exclude that fluorescently labeled E1 protein is
342 defective in assembling the viral envelope and that the composition of released viral particles
343 differs from unlabeled particles, we next employed biochemical assays.
344 E1 and E2 form heterodimers in the viral envelope (47, 48) and this process might be impeded
345 by fusion of E1 with mCherry. Using lysates from cells electroporated with Jc1-Flag-E2 (35) or
346 Jc1-E1(A4)-mCherry/Flag-E2 (see Figure 1A), that express a Flag-tagged E2 glycoprotein, we
347 performed immunoprecipitation (IP) against Flag. As expected, E1 precipitated with Flag-E2 and
348 more importantly interaction of E2 with E1 was not disrupted by the mCherry tag (Figure 2G).
349 HCV is a so-called lipo-viral particle (LVP) which results in a characteristic buoyant density
350 profile of released viral particles (35, 49). To investigate whether viral particles of Jc1-E1(A4)-
351 mCherry are assembled and released similarly to WT HCV Jc1 we fractionated supernatants
352 from Jc1-E1(A4) and Jc1-E1(A4)-mCherry-expressing cells and analyzed these fractions for the
353 presence of E2, E1(A4) and Core. The structural viral proteins of Jc1-E1(A4) as well as of Jc1-
354 E1(A4)-mCherry were present in the same fractions between 1.07 and 1.17 g/ml and peaked at
355 densities 1.13 (Jc1-E1(A4)) and 1.14 g/ml (Jc-E1(A4)-mCherry) (Fig. 2H) similar to the vRNA
356 genomes (Figure 2I). Importantly, this pattern coincides with detection of ApoE, which is most
357 abundant in fractions ranging from 1.08 to 1.16g/ml (Fig. 2H, lower panel). Hence, although Jc-
358 1E1(A4)-mCherry might have a slightly higher density presumably due to the mCherry tag, the
359 viral structural proteins appear in the same density fractions as the vRNA genomes and with the

specific density of infectious HCVcc particles (49). This strongly indicates authentic assembly and release of HCV Jc1-E1(A4)-mCherry which is comparable to untagged HCV Jc1-E1(A4). Altogether, the mCherry tag within E1 does not interfere with stable expression or intracellular localization of E1 or the other viral proteins tested. Furthermore, kinetics of viral protein expression and vRNA replication appear undisturbed by the tag and E1-mCherry interacts with E2. Most importantly, released viral particles tagged with E1-mCherry show similar growth kinetics and the same biochemical characteristics as WT HCV demonstrating authentic morphogenesis and secretion of our novel fluorescently labeled Jc1-E1(A4)-mCherry and Jc1-E1(A4)-mCherry/NS5A-GFP variants. Hence, the presented E1-mCherry tagged HCV Jc1 variants represent appropriate and unique tools to study the dynamics of HCV assembly and release in living cells.

Production of HCV structural protein and replication complexes appears to be tempo-spatially organized.

There is rapid appearance of replication complexes (RC) in HCV replicon expressing Huh7.5 cells visualized by NS5A-GFP and these RCs can be stable over several hours (50-52). Accordingly, we aimed to characterize the dynamics and formation of NS5A-GFP RCs and E1-mCherry structural protein accumulations, which could represent assembling or assembled viral particles in cells expressing full length HCV. Jc1-E1(A4)-mCherry/NS5A-GFP electroporated Huh7.5 cells were imaged over four days at the indicated time points starting at 24 hpe, when fluorescence emission from E1-mCherry and NS5A-GFP was detectable (Figure 3A). As expected, there was rapid formation of NS5A-GFP in RCs (50, 51) and E1-mCherry seemed to accumulate in distinct punctae in addition to the typical ER-associated expression pattern. From

383 the visual inspection of various images (see examples in Figure 3A), we got the impression of a
384 time-dependent decrease in RCs whereas E1-mCherry punctae seemed to accumulate. For
385 rigorous image quantification, we performed spot counting on multiple cells from independent
386 electroporations with an arbitrary threshold of 0.8 µm as maximum spot size (Figure 3B), which
387 is similar to previous analyses (50, 53). At 24 hpe, although E1-mCherry fluorescence was
388 readily detectable, there were only few punctae in comparison to the number of NS5A-GFP RCs.
389 Conversely, the number of E1-mCherry punctae increased 2.4-fold at 48 hpe compared to the 24
390 hpe time point and the number of RCs stayed constant (Figure 3B). At 72 and 96 hpe, the amount
391 of E1-mCherry punctae further increased or remained at the same level, whereas we observed a
392 continuous decline in the number of NS5A-GFP RCs (Figure 3B). Calculating the ratios of E1-
393 mCherry punctae to NS5A-GFP RCs for each cell over the 96 h observation period revealed a
394 continuous increase, suggesting that formation of RCs commences quickly after electroporation
395 and slows down over time while structural protein accumulations in the form of distinct punctae
396 are steadily increasing (Figure 3C).
397
398 **Time dependent increase in interaction of HCV E1-mCherry punctae with the other**
399 **structural proteins E2 and Core.**
400 The fact that the number of E1-mCherry punctae increases over time suggests that these punctae
401 might represent intracellular assembly sites of HCV particles. Since we expect intracellular
402 assembly sites to recruit the other structural proteins Core and E2, we analyzed the interaction of
403 E1-mCherry punctae with E2, Core and as controls NS3, and NS5A. Jc1-E1(A4)-mCherry
404 electroporated Huh7.5 cells were analyzed over a period of four days using proximity ligation
405 assay (PLA) as described previously (19) with E1-mCherry as primary PLA target and the other

406 viral proteins as putative interaction partners. Quantitative analysis of images such as those
407 shown in Figure 4A clearly demonstrated that E1-mCherry punctae interact with structural
408 proteins E2 and Core and that these interactions intensify over time (Figure 4B). The signals
409 were highly specific, since we did not detect a PLA signal when Jc1-E1(A4) electroporated
410 Huh7.5 cells were incubated with the same antibodies and PLA reagents (Figure 4B). In
411 addition, interaction of E1-mCherry with NS3 or NS5A was less pronounced, such that the
412 number of PLA punctae per cell slightly increased from 48-72 hpe but dropped again at later
413 time points. We would expect such a result assuming initial colocalization of E1 and NS5A at
414 the surface of lipid droplets during the formation of assembly sites followed by separation of
415 both proteins at the onset of viral assembly and release (Figure 4B). This finding is also in
416 accordance with our observations on punctae formation of E1-mCherry and NS5A-GFP (Figure
417 3B) and live cell imaging of Jc1-E1(A4)-mCherry/NS5A-GFP expressing Huh7.5 cells from 24
418 to 96 hpe (Supplemental Movies S1 – S6).
419
420 **E1-mCherry punctae are not detectable within the Golgi apparatus.**
421 E1-mCherry punctae, might to some extent represent assembled virions which are ready for
422 release or in the process of secretion (Figure 4). Therefore, colocalization analyses of E1-
423 mCherry punctae with markers of cellular pathways should be indicative for the HCV secretory
424 route. To investigate this, we first aimed to define the HCV secretory pathway by colocalization
425 studies and co-electroporated Huh7.5 cells with RNA of Jc1-E1(A4)-mCherry and vectors
426 encoding either GalT-CFP (Golgi), ApoE-GFP (lipoprotein trafficking) or CD74(Ii)-CFP (ER
427 and endosomal compartment) and analyzed these cells 56 hpe by confocal microscopy. As
428 expected, the bulk of E1-mCherry protein colocalized with the chaperone CD74, which is

429 located in the ER and endosomes/MVBs and with ApoE (Figure 5A). However, E1-mCherry
430 punctae did not colocalize with the Golgi-marker GalT (see line profiles in Figure 5A). To
431 exclude that the electroporation procedure might interfere with Golgi function or that there is an
432 as yet unknown Golgi defect in the used Huh7.5 cells, we co-electroporated vectors expressing
433 hepatitis B virus (HBV)-S-mCherry or Gaussia-luciferase-YFP, which are known to be secreted
434 through the Golgi apparatus (54, 55), together with the GalT-CFP fusion. Both proteins showed
435 strong colocalization with GalT-CFP as evident from the line profiles (Figure 5B), suggesting
436 intact Golgi function in Huh7.5 cells. In addition, the quantitative analyses of Pearsons
437 colocalization coefficient from multiple cells confirmed the absence of E1-mCherry detection
438 within the Golgi (GalT-CFP) and quantitatively corroborated colocalization with CD74 and
439 ApoE (Fig. 5C).
440
441 **HCV glycoproteins have a high mannose glycan structure.**
442 During secretion, Golgi residing enzymes process glycoproteins and modify asparagine-linked
443 mannose rich oligosaccharides into complex glycans. Complex glycans are resistant to treatment
444 with the endoglycosidase EndoH, but are cleaved by the peptide:*N*-glycosidase F (PNGaseF). By
445 implication, EndoH sensitivity of glycoproteins indicates high mannose glycans and absence of
446 glycoprotein modification by Golgi residing enzymes (56). We therefore assessed EndoH
447 sensitivity of cell- and virus-associated HCV E1 and E2 glycoproteins.
448 First, we verified proper processing of a Golgi secreted glycoprotein in Huh7.5 cells.
449 Supernatants from cells transfected to express the HBV-S glycoprotein were harvested, left
450 untreated, digested with PNGaseF or EndoH and subjected to WB analysis (Figure 6A). As

451 expected, HBV-S, which is secreted through the Golgi and therefore glycosylated in a complex
452 manner, was resistant to EndoH and could only be deglycosylated by PNGaseF (Figure 6A) (55).
453 We repeated the same experiment with lysates from cells that were electroporated with HCV
454 Jc1-E1(A4). In contrast to secreted HBV-S, cell-associated HCV E1 and E2 were sensitive to
455 EndoH and PNGaseF (Figure 6B) and we could observe deglycosylation of E1 and E2 in a dose-
456 dependent manner for both enzymes (Figure 6C).
457 It is possible that Golgi enzymes only modify a small fraction of E1 and E2 and that this fraction
458 is incorporated into released viral particles. Hence, we harvested the supernatants of HCV
459 Jc1(A4) expressing Huh7.5 cells which were concentrated by ultracentrifugation and fractionated
460 by a iodixanol gradient prior to treatment with EndoH and PNGaseF (Figure 6D). Of note, E1
461 and E2 in fraction 3 displayed a partly EndoH resistant phenotype. However, based on the
462 absence of detectable HCV Core this fraction does not appear to contain significant amounts of
463 assembled particles. Conversely, E1 and E2 associated with the vast majority of assembled virus
464 particles in fraction 5 (as well as in all other fractions) were fully sensitive towards EndoH
465 digestion (Figure 6D). In conclusion, the majority of HCV glycoproteins E1 and E2 associated
466 with assembled and released viral particles have not been modified by Golgi residing enzymes
467 and exhibit a high-mannose glycan structure.
468
469 **HCV E1-mCherry punctae traffic with Rab9A-positive compartments.**
470 Since E1-mCherry punctae were not associated with Golgi structures, but partly colocalized with
471 ApoE and CD74 (Figure 5), we aimed to identify intracellular trafficking compartments,
472 potentially involved in HCV release. Previously, involvement of the endosomal compartment in
473 HCV Core trafficking was postulated (25, 57-59). Hence, we co-electroporated Huh7.5 cells with

RNA of HCV Jc1-E1(A4)-mCherry and vectors encoding Rab7A-CFP or Rab9A-CFP and VSV-G-GFP as a control glycoprotein that is known to traffic through the Golgi during maturation (60). Rab7A and Rab9A are cellular proteins that have roles in late endosomal trafficking (61). Colocalization of E1-mCherry and the indicated proteins was analyzed 48 hpe by line profiling. Consistent with our previous results (Figure 5) we did not observe any colocalization of E1-mCherry with VSV-G-GFP (Figure 7A, top row). In contrast, few E1-mCherry punctae appeared to colocalize with Rab7A-CFP and Rab9A-CFP (Figure 7A, mid and bottom rows).

Assembling HCV particles might be connected to sites of viral protein translation and trafficking whereas assembled particles are most likely present in membrane-enclosed transport compartments. We first explored the nature of intracellular E1-mCherry punctae with fluorescence recovery after photobleaching (FRAP) and indeed confirmed the presence of different types of E1-mCherry punctae that either stayed bleached or could recover fluorescence to some extent (Supplemental Movie S7). This supports our hypothesis of assembled viral particles within membrane-enclosed compartments. The endosomal compartment, and more specifically Rab9A-positive vesicles could be part of such an intracellular trafficking pathway. Hence, we repeated FRAP with Huh7.5 cells co-electroporated with HCV Jc1-E1(A4)-mCherry RNA and a vector encoding Rab9A-CFP (Figure 7B and Supplemental Movie S8). When we specifically bleached a Rab9A-negative E1-mCherry puncta, E1-mCherry fluorescence recovered to nearly 60 % within 300 s (Figure 7C). In contrast, the E1-mCherry fluorescence of a puncta positive for Rab9A-CFP did not recover (Figures 7B and C).

Altogether, this data indicates that intracellular trafficking of E1-mCherry, which might be associated with assembled HCV particles, involves the endosomal compartment and more specifically Rab9A-positive vesicles.

497

498 **Inhibition of the early endosomal pathway suppresses HCV release.**

499 Our data indicates that HCV release involves the endosomal compartment. To assess this in a
500 quantitative manner, we used U18666A that inhibits intracellular movement of endosomes
501 through blocking the cholesterol *de novo* synthesis and transport of LDL-derived cholesterol (62,
502 63). Of note, while prolonged incubation with U18666A for 48 hours or longer suppresses HCV
503 RNA replication (64), shorter incubation periods have no such effect and were previously used to
504 inhibit HCV release (57). We therefore electroporated Huh7.5 cells with RNA of HCV Jc1-luc
505 (34) and incubated the cells with U18666A at 48 hpe for eight hours. For a positive control, we
506 included BrefeldinA that completely blocks vesicular protein transport from the ER (65, 66). We
507 then cleared HCV-luc containing supernatants by sucrose centrifugation and used them to infect
508 native Huh7.5 cells to quantify infectious virus particle release by luciferase activity in cell
509 lysates (Figure 8A). To directly compare the effects of the inhibitor on a cargo that is released
510 via secretion through the Golgi, we used Huh7.5 cells, which were electroporated with a plasmid
511 encoding Gaussia luciferase (37, 54). This approach directly allows to assess the efficiency of
512 Gaussia secretion by measurement of luciferase activity in the supernatant (Figure 8B). Addition
513 of Brefeldin A completely blocked HCV and Gaussia release (Figures 8A and B) and this effect
514 was reversible (data not shown). However, as reported before (67), we also noticed that
515 Brefeldin A had an inhibiting effect on intracellular levels of HCV associated luciferase activity,
516 and hence most likely on viral RNA replication (Fig. 8A, lower panel). On the contrary,
517 U18666A completely inhibited HCV release (Figure 8A), but only marginally affected Gaussia
518 secretion (Figures 8B). This effect was specific for release, since the concentration of U18666A

used here (25 μM) had no inhibitory effect on intracellular virus production (Fig. 8A, lower panel).

In general, inhibitors including U18666A, might have non-specific side effects. Hence, we applied an independent technique for specific inhibition of the early endosomal pathway based on biochemical fixation of endosomes (44, 45). Huh7.5 cells electroporated with RNA of HCV Jc1-luc or transfected to express Gaussia luciferase were fed with horseradish peroxidase (HRP) coupled to transferrin (Tf), which is taken up into the early endosomal pathway. Addition of the HRP substrate DAB chemically fixes endosomes within living cells, thus inactivates the endosomal pathway without damaging the cells. After inactivation of endosomes we allowed the cells to produce virus/Gaussia-luciferase into the supernatant for eight hours and then measured supernatant associated infectivity with the HCV Jc1-luc (Figure 8C) or Gaussia-luciferase activity (Figure 8D). Inactivation of endosomes strongly suppressed HCV release in comparison to control cells, that were treated identically but fed with Tf instead of HRP-TF (Figure 8D). Strikingly, the release of Gaussia luciferase was not affected by fixation of early endosomes (Figure 8D) and the procedure had no negative effects on intracellular levels of HCV or Gaussia (Fig. 8C and D, lower panels). From the comparative analysis of HCV versus Gaussia release (Fig. 8E), we conclude that the endosomal pathway is integral to HCV release and that secretion of viral particles differs from the canonical secretory route.

DISCUSSION

Here, we establish and exploit fluorescently labeled HCV genomes to study intracellular viral trafficking and the dynamics of structural and non-structural protein expression. HCV genomes or replicons containing a GFP tag within NS5A were described previously and successfully used

542 to analyze intracellular movement of the replication complex and to investigate HCV
543 superinfection (33, 50, 52, 68). In contrast to this, our novel HCV Jc1 variants containing
544 mCherry within E1 allow to track intracellular distribution of a structural protein and its
545 movement and are alternatives to the HCV genomes with a tetracystein tag in Core (30, 53).
546 Core is post-translationally processed and is targeted towards the ER through its C-terminus (18,
547 69). Furthermore it contains important *cis*-active elements to regulate and initiate polyprotein
548 translation (70) and plays a crucial role in assembly and release (8, 18, 71). We therefore chose
549 to introduce the tag into one of the envelope proteins of HCV. Since, E2 mediates attachment to
550 cellular receptors and shields E1 in a heteromeric complex (1, 72), we inserted mCherry between
551 the C-terminal glycosylation site and the N-terminus of the transmembrane domain of E1. While
552 the tag unfortunately reduced infectivity (Fig. 2B), Jc1-E1(A4)-mCherry and Jc1-E1(A4)-
553 mCherry/NS5A-GFP showed normal levels of polyprotein expression and processing.
554 Furthermore, comprehensive biochemical analyses demonstrated release of HCV particles from
555 the fluorescently labeled genomes with a similar buoyant density as compared to untagged HCV
556 Jc1 (49) and in conjunction with apolipoprotein (22). Taken together, apart from reduced
557 infectivity, most likely due to structural alterations of the envelope glycoprotein complex, our
558 novel E1-mCherry tagged HCV genomes show properties comparable to WT HCV and hence
559 represent unique and valuable tools to investigate viral morphogenesis, assembly, budding and
560 egress.
561 We found a temporal and spatial regulation of structural E1-mCherry and non-structural NS5A-
562 GFP expression. NS5A was rapidly expressed and localized to punctae most likely representing
563 RCs (50-52). In contrast, E1-mCherry localization was initially rather dispersed and then
564 accumulated in punctae over the four day observation period (Fig. 3 and Supplemental Movies

565 S1 – S6). Dynamic formation of NS5A RCs and punctae containing structural protein Core has
566 been reported before and the results are in agreement with our data (30, 50, 52, 53). However,
567 previous studies did not assess formation dynamics over such a long period and had not the
568 opportunity to monitor the kinetics of E1 and NS5A simultaneously, as it is now feasible with
569 our double-labeled genome. Furthermore, using PLA in conjunction with localization
570 microscopy allowed to specifically analyze time dependent interaction of HCV proteins within
571 the E1-mCherry punctae (Figure 4). The temporal increase in E1-mCherry punctae interacting
572 with the other envelope glycoprotein E2, as well as with the capsid protein Core strongly
573 supports the identity of E1-mCherry punctae as sites of ongoing HCV assembly or assembled
574 virions. In addition, E1-mCherry punctae transiently interact with NS proteins (NS3 and NS5A)
575 at 48 hpe and NS5A-GFP RCs decrease from 48 to 96 hpe (Figure 3). In conclusion, viral
576 replication and translation appears to be initiated rapidly after delivery of viral RNA into the
577 cytoplasm followed by a continuous increase in structural protein interactions, possibly
578 resembling the formation of viral particles. In parallel, RCs continuously decrease, which could
579 reflect a shutdown of vRNA replication and viral protein translation (51).
580 Conceivably, detection of E1-mCherry punctae at later time points is indicative for intracellular
581 transport pathways exploited by viral particles. Analyses of cells from 56 to 72 hpe revealed that
582 E1-mCherry punctae are part of the endosomal compartment and do not carry Golgi markers or
583 colocalize with Golgi secreted proteins (Figures 5 and 7). Others have reported trafficking of
584 HCV Core in endosomal compartments (57), however, it was not clear if this proportion of Core
585 is indicative of assembled virions or Core protein accumulations alone. Glenn Randalls group
586 performed non-quantitative colocalization analysis and even though their results look very
587 similar to ours they were interpreted in a different way, arguing for a small sub-proportion of

structural protein trafficking through the Golgi (30). We have to acknowledge, that the presence of such markers is often ambiguous, semi-quantitative and gives room for various interpretations. Therefore, we used inhibitors targeting cellular transport pathways and performed biochemical characterization of released HCV particles. Brefeldin A completely blocked the release of infectious particles which is not surprising, since Brefeldin A is a broad spectrum inhibitor and disrupts trafficking from the ER to the Golgi, to the endosomal compartment and vesicle formation at the plasma membrane (65, 66) as well as HCV RNA replication (73). Conversely, HCV release was suppressed by U18666A, an inhibitor of endosomal trafficking (62), and in an independent experimental setting in which we biochemically fixed early endosomes within HCV infected Huh7.5 cells. In sum, the different independent lines of evidence presented here support the conclusion that intracellular vesicles containing assembled HCV are part of the endosomal compartment. This is in agreement with another study showing Core trafficking in endosomes (57) and corroborated by reports demonstrating the involvement of key components of the endosomal machinery ESCRT-III, Vps4, TIP47 and Rab9A in HCV production and release (74-77).

Intriguingly, EndoH cleaves glycans of E1 and E2 envelope glycoproteins present in the vast majority of released viral particles (Figure 6). This demonstrates that the bulk of E1 and E2 is not processed by Golgi residing enzymes during release and gives rise to the question whether assembled HCV is secreted through the Golgi. Here we propose a non-canonical secretory route for the majority of assembled HCV particles. We base this hypothesis on three lines of evidence: (i) HCV E1-mCherry punctae do not colocalize with Golgi markers; (ii) Inhibition of the endosomal compartment specifically inhibits HCV egress but not release of the Golgi-secreted Gaussia-luciferase; (iii) Glycoproteins on released HCV particles are sensitive to EndoH.

611 Our model is not at odds with studies postulating an important role of the Golgi for HCV release
612 (29, 30, 78). It is well conceivable that Golgi-derived factors or Golgi components are important
613 for assembly and/or participate in the release of assembled particles. However, this does not
614 necessarily imply release of assembled virus via the canonical Golgi-mediated secretory route.
615 Our data is also in accordance with the work of Dubuisson and coworkers (48). In this study they
616 observed, similar to our results, that the bulk of E1 glycoprotein in the whole supernatant of cell
617 culture produced HCV (HCVcc) was EndoH sensitive and E2 was partly resistant. In line, our
618 data shows that a fraction of E1 and E2 was EndoH resistant (density of 1.06 to 1.08 g/ml;
619 fraction 3, comp. Figure 6D). Although this fraction might only resemble the minority of
620 assembled and released particles, based on the low amounts of glycoprotein as well as Core, it is
621 well known that particles of this density are highly infectious (49). In conclusion, despite the
622 observation that the bulk of HCV particles takes an alternative route, the canonical secretory
623 pathway might still give rise to infectious HCV progeny to some degree. The use of a non-
624 canonical pathway by HCV is also compatible with the finding by the Dubuisson group showing
625 that glycoproteins incorporated into HCV pseudoparticles (HCVpp) are EndoH resistant (48). Of
626 note, HCVpp are HIV-1 particles produced from 293T cells which incorporate HCV envelope
627 proteins (79). HCVpps are assembled at the plasma membrane whereas HCV virions are
628 assembled at the ER close to lipid droplets (LDs) (8, 13). Thus, it is tempting to speculate that
629 the cellular localization of particle assembly determines whether E1 and E2 proteins are
630 modified by Golgi enzymes. Most likely, HCVcc particles incorporate glycoproteins at the ER
631 close to LDs before Golgi passage, whereas HCVpp particles need to incorporate E1 and E2 at
632 the plasma membrane post trafficking through the Golgi.

One key question and unresolved issue remains regarding the exact identity of the non-canonical secretory route taken by HCV. The most provocative hypothesis would be the presence of a not yet discovered secretory route bypassing the Golgi and allowing direct secretion of proteins from the ER and ER-convoluted membranes to the plasma membrane. Such a mechanism is possible, given the fact that Golgi-bypass has been described in the literature before (80). Furthermore, rotaviruses are known to bypass the Golgi during assembly and release, although the mechanisms are poorly understood and the biology of this virus strongly differs from HCV (81). Other possible explanations for the phenotypes we observe are virus-induced alterations of the Golgi-complex including its dispersion as proposed (25, 29) or classical secretion without processing of the HCV glycoproteins by Golgi residing enzymes due to their putative inaccessibility when associated with lipids (35). Given the fact that a proportion of HCV glycoproteins indeed carries complex glycans (48) (Figure 6D) and Golgi function is essential for cellular survival, complete Golgi dispersion seems unlikely and the differential egress of HCV versus Golgi secreted Gaussia-luciferase (Figure 8) indeed argues for an alternative pathway of release.

In sum, this study established HCV viral genomes encoding fluorescently labeled viral proteins, which were exploited to characterize the pathway of HCV release. We discovered a non-canonical and as yet unknown route of HCV secretion from Huh7.5 cells involving the endosomal pathway. In the future, it will be important and highly relevant to further characterize this secretory pathway and delineate if it is induced by HCV to initiate release or if it is an intrinsic property of the cell.

ACKNOWLEDGMENTS

656 We would like to thank Ulrike Protzer, Gerhard Jahn and Thomas Iftner for constant support and
657 encouragement. Most importantly, this work would have never been possible without the
658 generous gift of many essential reagents contributed by various researchers. We would especially
659 like to thank Ralf Bartenschlager, Charles Rice, Takashi Wakita, Glenn Randall, Harry
660 Greenberg, Franck Perez, Andrea Musacchio, Philippe Bastiaens, Dieter Glebe and Genentech
661 for their kind help (see Materials and Methods). Furthermore we would like to acknowledge
662 Gabrielle Vieyres and Thomas Pietschmann for fruitful and helpful discussions and critical
663 reading of the manuscript.

664

665 **REFERENCES**

666 1. **Moradpour D, Penin F, Rice CM.** 2007. Replication of hepatitis C virus. Nature reviews
667 Microbiology **5:**453-463.
668 2. **Gouttenoire J, Penin F, Moradpour D.** 2010. Hepatitis C virus nonstructural protein
669 4B: a journey into unexplored territory. Reviews in medical virology **20:**117-129.
670 3. **Romero-Brey I, Merz A, Chiramel A, Lee JY, Chlanda P, Haselman U, Santarella-**
671 **Mellwig R, Habermann A, Hoppe S, Kallis S, Walther P, Antony C, Krijnse-Locker**
672 **J, Bartenschlager R.** 2012. Three-dimensional architecture and biogenesis of membrane
673 structures associated with hepatitis C virus replication. PLoS Pathog **8:**e1003056.
674 4. **Egger D, Wolk B, Gosert R, Bianchi L, Blum HE, Moradpour D, Bienz K.** 2002.
675 Expression of hepatitis C virus proteins induces distinct membrane alterations including a
676 candidate viral replication complex. J Virol **76:**5974-5984.

5. **Gosert R, Egger D, Lohmann V, Bartenschlager R, Blum HE, Bienz K, Moradpour D.** 2003. Identification of the hepatitis C virus RNA replication complex in Huh-7 cells harboring subgenomic replicons. J Virol **77:**5487-5492.

6. **Boulant S, Montserret R, Hope RG, Ratinier M, Targett-Adams P, Lavergne JP, Penin F, McLauchlan J.** 2006. Structural determinants that target the hepatitis C virus core protein to lipid droplets. The Journal of biological chemistry **281:**22236-22247.

7. **Boulant S, Targett-Adams P, McLauchlan J.** 2007. Disrupting the association of hepatitis C virus core protein with lipid droplets correlates with a loss in production of infectious virus. The Journal of general virology **88:**2204-2213.

8. **Miyanari Y, Atsuzawa K, Usuda N, Watashi K, Hishiki T, Zayas M, Bartenschlager R, Wakita T, Hijikata M, Shimotohno K.** 2007. The lipid droplet is an important organelle for hepatitis C virus production. Nature cell biology **9:**1089-1097.

9. **Cocquerel L, Meunier JC, Pillez A, Wychowski C, Dubuisson J.** 1998. A retention signal necessary and sufficient for endoplasmic reticulum localization maps to the transmembrane domain of hepatitis C virus glycoprotein E2. Journal of virology **72:**2183-2191.

10. **Cocquerel L, Duvet S, Meunier JC, Pillez A, Cacan R, Wychowski C, Dubuisson J.** 1999. The transmembrane domain of hepatitis C virus glycoprotein E1 is a signal for static retention in the endoplasmic reticulum. Journal of virology **73:**2641-2649.

11. **Popescu CI, Callens N, Trinel D, Roingeard P, Moradpour D, Descamps V, Duverlie G, Penin F, Heliot L, Rouille Y, Dubuisson J.** 2011. NS2 protein of hepatitis C virus interacts with structural and non-structural proteins towards virus assembly. PLoS Pathog **7:**e1001278.

12. **Stapleford KA, Lindenbach BD.** 2011. Hepatitis C virus NS2 coordinates virus particle assembly through physical interactions with the E1-E2 glycoprotein and NS3-NS4A enzyme complexes. J Virol **85:**1706-1717.

13. **Bartenschlager R, Penin F, Lohmann V, Andre P.** 2011. Assembly of infectious hepatitis C virus particles. Trends Microbiol **19:**95-103.

14. **Oakland TE, Haselton KJ, Randall G.** 2013. EWSR1 binds the hepatitis C virus cis-acting replication element and is required for efficient viral replication. J Virol **87:**6625-6634.

15. **Herker E, Harris C, Hernandez C, Carpentier A, Kaehlcke K, Rosenberg AR, Farese RV, Jr., Ott M.** 2010. Efficient hepatitis C virus particle formation requires diacylglycerol acyltransferase-1. Nature medicine **16:**1295-1298.

16. **Camus G, Vogt DA, Kondratowicz AS, Ott M.** 2013. Lipid droplets and viral infections. Methods Cell Biol **116:**167-190.

17. **Popescu CI, Callens N, Trinel D, Roingeard P, Moradpour D, Descamps V, Duverlie G, Penin F, Heliot L, Rouille Y, Dubuisson J.** 2011. NS2 protein of hepatitis C virus interacts with structural and non-structural proteins towards virus assembly. PLoS pathogens **7:**e1001278.

18. **Boson B, Granio O, Bartenschlager R, Cosset FL.** 2011. A concerted action of hepatitis C virus p7 and nonstructural protein 2 regulates core localization at the endoplasmic reticulum and virus assembly. PLoS pathogens **7:**e1002144.

19. **Hagen N, Bayer K, Rosch K, Schindler M.** 2014. The intraviral protein interaction network of hepatitis C virus. Mol Cell Proteomics **13:**1676-1689.

722 20. **Benga WJ, Krieger SE, Dimitrova M, Zeisel MB, Parnot M, Lupberger J, Hildt E,**
723 **Luo G, McLauchlan J, Baumert TF, Schuster C.** 2010. Apolipoprotein E interacts with
724 hepatitis C virus nonstructural protein 5A and determines assembly of infectious particles.
725 Hepatology **51:**43-53.
726 21. **Boyer A, Dumans A, Beaumont E, Etienne L, Roingeard P, Meunier JC.** 2014. The
727 association of hepatitis C virus glycoproteins with apolipoproteins E and B early in
728 assembly is conserved in lipoviral particles. J Biol Chem **289:**18904-18913.
729 22. **Lee JY, Acosta EG, Stoeck IK, Long G, Hiet MS, Mueller B, Fackler OT, Kallis S,**
730 **Bartenschlager R.** 2014. Apolipoprotein E likely contributes to a maturation step of
731 infectious hepatitis C virus particles and interacts with viral envelope glycoproteins. J
732 Virol **88:**12422-12437.
733 23. **Li X, Jiang H, Qu L, Yao W, Cai H, Chen L, Peng T.** 2014. Hepatocyte nuclear factor
734 4alpha and downstream secreted phospholipase A2 GXIIB regulate production of
735 infectious hepatitis C virus. J Virol **88:**612-627.
736 24. **Bartenschlager R, Penin F, Lohmann V, Andre P.** 2011. Assembly of infectious
737 hepatitis C virus particles. Trends in microbiology **19:**95-103.
738 25. **Mankouri J, Walter C, Stewart H, Bentham M, Park WS, Heo WD, Fukuda M,**
739 **Griffin S, Harris M.** 2016. Release of Infectious Hepatitis C Virus from Huh7 Cells
740 Occurs via a trans-Golgi Network-to-Endosome Pathway Independent of Very-Low-
741 Density Lipoprotein Secretion. J Virol **90:**7159-7170.
742 26. **Chambers TJ, Hahn CS, Galler R, Rice CM.** 1990. Flavivirus genome organization,
743 expression, and replication. Annual review of microbiology **44:**649-688.

744 27. **Welsch S, Miller S, Romero-Brey I, Merz A, Bleck CK, Walther P, Fuller SD,**
745 **Antony C, Krijnse-Locker J, Bartenschlager R.** 2009. Composition and three-
746 dimensional architecture of the dengue virus replication and assembly sites. Cell host &
747 microbe **5:**365-375.
748 28. **Weiskircher E, Aligo J, Ning G, Konan KV.** 2009. Bovine viral diarrhea virus NS4B
749 protein is an integral membrane protein associated with Golgi markers and rearranged
750 host membranes. Virology journal **6:**185.
751 29. **Bishe B, Syed GH, Field SJ, Siddiqui A.** 2012. Role of phosphatidylinositol 4-phosphate
752 (PI4P) and its binding protein GOLPH3 in hepatitis C virus secretion. J Biol Chem
753 **287:**27637-27647.
754 30. **Coller KE, Heaton NS, Berger KL, Cooper JD, Saunders JL, Randall G.** 2012.
755 Molecular determinants and dynamics of hepatitis C virus secretion. PLoS Pathog
756 **8:**e1002466.
757 31. **Vieyres G, Dubuisson J, Pietschmann T.** 2014. Incorporation of hepatitis C virus E1
758 and E2 glycoproteins: the keystones on a peculiar virion. Viruses **6:**1149-1187.
759 32. **Scott KL, Kabbarah O, Liang MC, Ivanova E, Anagnostou V, Wu J, Dhakal S, Wu**
760 **M, Chen S, Feinberg T, Huang J, Saci A, Widlund HR, Fisher DE, Xiao Y, Rimm**
761 **DL, Protopopov A, Wong KK, Chin L.** 2009. GOLPH3 modulates mTOR signalling
762 and rapamycin sensitivity in cancer. Nature **459:**1085-1090.
763 33. **Schaller T, Appel N, Koutsoudakis G, Kallis S, Lohmann V, Pietschmann T,**
764 **Bartenschlager R.** 2007. Analysis of hepatitis C virus superinfection exclusion by using
765 novel fluorochrome gene-tagged viral genomes. J Virol **81:**4591-4603.

766 34. **Pietschmann T, Kaul A, Koutsoudakis G, Shavinskaya A, Kallis S, Steinmann E,**
767 **Abid K, Negro F, Dreux M, Cosset FL, Bartenschlager R.** 2006. Construction and
768 characterization of infectious intragenotypic and intergenotypic hepatitis C virus
769 chimeras. Proceedings of the National Academy of Sciences of the United States of
770 America **103:**7408-7413.
771 35. **Merz A, Long G, Hiet MS, Brugger B, Chlanda P, Andre P, Wieland F, Krijnse-**
772 **Locker J, Bartenschlager R.** 2011. Biochemical and morphological properties of
773 hepatitis C virus particles and determination of their lipidome. J Biol Chem **286:**3018-
774 3032.
775 36. **Dubuisson J, Hsu HH, Cheung RC, Greenberg HB, Russell DG, Rice CM.** 1994.
776 Formation and intracellular localization of hepatitis C virus envelope glycoprotein
777 complexes expressed by recombinant vaccinia and Sindbis viruses. J Virol **68:**6147-6160.
778 37. **Tannous BA, Kim DE, Fernandez JL, Weissleder R, Breakefield XO.** 2005. Codon-
779 optimized Gaussia luciferase cDNA for mammalian gene expression in culture and in
780 vivo. Molecular therapy : the journal of the American Society of Gene Therapy **11:**435-
781 443.
782 38. **Banning C, Votteler J, Hoffmann D, Koppensteiner H, Warmer M, Reimer R,**
783 **Kirchhoff F, Schubert U, Hauber J, Schindler M.** 2010. A flow cytometry-based FRET
784 assay to identify and analyse protein-protein interactions in living cells. PloS one **5:**e9344.
785 39. **Rocks O, Gerauer M, Vartak N, Koch S, Huang ZP, Pechlivanis M, Kuhlmann J,**
786 **Brunsveld L, Chandra A, Ellinger B, Waldmann H, Bastiaens PI.** 2010. The
787 palmitoylation machinery is a spatially organizing system for peripheral membrane
788 proteins. Cell **141:**458-471.

40. **Blight KJ, McKeating JA, Rice CM.** 2002. Highly permissive cell lines for subgenomic and genomic hepatitis C virus RNA replication. Journal of virology **76:**13001-13014.

41. **Wakita T, Pietschmann T, Kato T, Date T, Miyamoto M, Zhao Z, Murthy K, Habermann A, Krausslich HG, Mizokami M, Bartenschlager R, Liang TJ.** 2005. Production of infectious hepatitis C virus in tissue culture from a cloned viral genome. Nature medicine **11:**791-796.

42. **Kato T, Date T, Murayama A, Morikawa K, Akazawa D, Wakita T.** 2006. Cell culture and infection system for hepatitis C virus. Nature protocols **1:**2334-2339.

43. **Owsianka A, Tarr AW, Juttla VS, Lavillette D, Bartosch B, Cosset FL, Ball JK, Patel AH.** 2005. Monoclonal antibody AP33 defines a broadly neutralizing epitope on the hepatitis C virus E2 envelope glycoprotein. Journal of virology **79:**11095-11104.

44. **Brachet V, Pehau-Arnaudet G, Desaymard C, Raposo G, Amigorena S.** 1999. Early endosomes are required for major histocompatiblity complex class II transport to peptide-loading compartments. Molecular biology of the cell **10:**2891-2904.

45. **Pond L, Watts C.** 1997. Characterization of transport of newly assembled, T cell-stimulatory MHC class II-peptide complexes from MHC class II compartments to the cell surface. Journal of immunology **159:**543-553.

46. **Shaner NC, Campbell RE, Steinbach PA, Giepmans BN, Palmer AE, Tsien RY.** 2004. Improved monomeric red, orange and yellow fluorescent proteins derived from Discosoma sp. red fluorescent protein. Nature biotechnology **22:**1567-1572.

47. **Deleersnyder V, Pillez A, Wychowski C, Blight K, Xu J, Hahn YS, Rice CM, Dubuisson J.** 1997. Formation of native hepatitis C virus glycoprotein complexes. J Virol **71:**697-704.

812 48. **Vieyres G, Thomas X, Descamps V, Duverlie G, Patel AH, Dubuisson J.** 2010.
813 Characterization of the envelope glycoproteins associated with infectious hepatitis C
814 virus. J Virol **84:**10159-10168.
815 49. **Gastaminza P, Kapadia SB, Chisari FV.** 2006. Differential biophysical properties of
816 infectious intracellular and secreted hepatitis C virus particles. J Virol **80:**11074-11081.
817 50. **Wolk B, Buchele B, Moradpour D, Rice CM.** 2008. A dynamic view of hepatitis C
818 virus replication complexes. J Virol **82:**10519-10531.
819 51. **Shulla A, Randall G.** 2015. Spatiotemporal analysis of hepatitis C virus infection. PLoS
820 Pathog **11:**e1004758.
821 52. **Eyre NS, Fiches GN, Aloia AL, Helbig KJ, McCartney EM, McErlean CS, Li K,**
822 **Aggarwal A, Turville SG, Beard MR.** 2014. Dynamic imaging of the hepatitis C virus
823 NS5A protein during a productive infection. J Virol **88:**3636-3652.
824 53. **Counihan NA, Rawlinson SM, Lindenbach BD.** 2011. Trafficking of hepatitis C virus
825 core protein during virus particle assembly. PLoS Pathog **7:**e1002302.
826 54. **Niers JM, Kerami M, Pike L, Lewandrowski G, Tannous BA.** 2011. Multimodal in
827 vivo imaging and blood monitoring of intrinsic and extrinsic apoptosis. Mol Ther
828 **19:**1090-1096.
829 55. **Chua PK, Wang RY, Lin MH, Masuda T, Suk FM, Shih C.** 2005. Reduced secretion
830 of virions and hepatitis B virus (HBV) surface antigen of a naturally occurring HBV
831 variant correlates with the accumulation of the small S envelope protein in the
832 endoplasmic reticulum and Golgi apparatus. J Virol **79:**13483-13496.
833 56. **Stanley P.** 2011. Golgi glycosylation. Cold Spring Harb Perspect Biol **3**.

57. **Lai CK, Jeng KS, Machida K, Lai MM.** 2010. Hepatitis C virus egress and release depend on endosomal trafficking of core protein. J Virol **84:**11590-11598.

58. **Benedicto I, Gondar V, Molina-Jimenez F, Garcia-Buey L, Lopez-Cabrera M, Gastaminza P, Majano PL.** 2015. Clathrin mediates infectious hepatitis C virus particle egress. J Virol **89:**4180-4190.

59. **Lai CK, Saxena V, Tseng CH, Jeng KS, Kohara M, Lai MM.** 2014. Nonstructural protein 5A is incorporated into hepatitis C virus low-density particle through interaction with core protein and microtubules during intracellular transport. PLoS One **9:**e99022.

60. **Presley JF, Cole NB, Schroer TA, Hirschberg K, Zaal KJ, Lippincott-Schwartz J.** 1997. ER-to-Golgi transport visualized in living cells. Nature **389:**81-85.

61. **Barbero P, Bittova L, Pfeffer SR.** 2002. Visualization of Rab9-mediated vesicle transport from endosomes to the trans-Golgi in living cells. J Cell Biol **156:**511-518.

62. **Liscum L, Faust JR.** 1989. The intracellular transport of low density lipoprotein-derived cholesterol is inhibited in Chinese hamster ovary cells cultured with 3-beta-[2-(diethylamino)ethoxy]androst-5-en-17-one. The Journal of biological chemistry **264:**11796-11806.

63. **Gatta AT, Wong LH, Sere YY, Calderon-Norena DM, Cockcroft S, Menon AK, Levine TP.** 2015. A new family of StART domain proteins at membrane contact sites has a role in ER-PM sterol transport. Elife **4**.

64. **Takano T, Tsukiyama-Kohara K, Hayashi M, Hirata Y, Satoh M, Tokunaga Y, Tateno C, Hayashi Y, Hishima T, Funata N, Sudoh M, Kohara M.** 2011. Augmentation of DHCR24 expression by hepatitis C virus infection facilitates viral replication in hepatocytes. J Hepatol **55:**512-521.

65. **Hunziker W, Whitney JA, Mellman I.** 1992. Brefeldin A and the endocytic pathway. Possible implications for membrane traffic and sorting. FEBS letters **307:**93-96.

66. **Saenz JB, Sun WJ, Chang JW, Li J, Bursulaya B, Gray NS, Haslam DB.** 2009. Golgicide A reveals essential roles for GBF1 in Golgi assembly and function. Nat Chem Biol **5:**157-165.

67. **Goueslain L, Alsaleh K, Horellou P, Roingeard P, Descamps V, Duverlie G, Ciczora Y, Wychowski C, Dubuisson J, Rouille Y.** 2010. Identification of GBF1 as a cellular factor required for hepatitis C virus RNA replication. J Virol **84:**773-787.

68. **Moradpour D, Evans MJ, Gosert R, Yuan Z, Blum HE, Goff SP, Lindenbach BD, Rice CM.** 2004. Insertion of green fluorescent protein into nonstructural protein 5A allows direct visualization of functional hepatitis C virus replication complexes. J Virol **78:**7400-7409.

69. **McLauchlan J, Lemberg MK, Hope G, Martoglio B.** 2002. Intramembrane proteolysis promotes trafficking of hepatitis C virus core protein to lipid droplets. The EMBO journal **21:**3980-3988.

70. **Vassilaki N, Friebe P, Meuleman P, Kallis S, Kaul A, Paranhos-Baccala G, Leroux-Roels G, Mavromara P, Bartenschlager R.** 2008. Role of the hepatitis C virus core+1 open reading frame and core cis-acting RNA elements in viral RNA translation and replication. Journal of virology **82:**11503-11515.

71. **Ait-Goughoulte M, Hourioux C, Patient R, Trassard S, Brand D, Roingeard P.** 2006. Core protein cleavage by signal peptide peptidase is required for hepatitis C virus-like particle assembly. The Journal of general virology **87:**855-860.

72. **Lavie M, Goffard A, Dubuisson J.** 2007. Assembly of a functional HCV glycoprotein heterodimer. Current issues in molecular biology **9:**71-86.

73. **Matto M, Sklan EH, David N, Melamed-Book N, Casanova JE, Glenn JS, Aroeti B.** 2011. Role for ADP ribosylation factor 1 in the regulation of hepatitis C virus replication. Journal of virology **85:**946-956.

74. **Corless L, Crump CM, Griffin SD, Harris M.** 2010. Vps4 and the ESCRT-III complex are required for the release of infectious hepatitis C virus particles. The Journal of general virology **91:**362-372.

75. **Ariumi Y, Kuroki M, Maki M, Ikeda M, Dansako H, Wakita T, Kato N.** 2011. The ESCRT system is required for hepatitis C virus production. PloS one **6:**e14517.

76. **Ploen D, Hafirassou ML, Himmelsbach K, Sauter D, Biniossek ML, Weiss TS, Baumert TF, Schuster C, Hildt E.** 2013. TIP47 plays a crucial role in the life cycle of hepatitis C virus. J Hepatol **58:**1081-1088.

77. **Ploen D, Hafirassou ML, Himmelsbach K, Schille SA, Biniossek ML, Baumert TF, Schuster C, Hildt E.** 2013. TIP47 is associated with the hepatitis C virus and its interaction with Rab9 is required for release of viral particles. Eur J Cell Biol **92:**374-382.

78. **Menzel N, Fischl W, Hueging K, Bankwitz D, Frentzen A, Haid S, Gentzsch J, Kaderali L, Bartenschlager R, Pietschmann T.** 2012. MAP-kinase regulated cytosolic phospholipase A2 activity is essential for production of infectious hepatitis C virus particles. PLoS Pathog **8:**e1002829.

79. **Bartosch B, Dubuisson J, Cosset FL.** 2003. Infectious hepatitis C virus pseudo-particles containing functional E1-E2 envelope protein complexes. The Journal of experimental medicine **197:**633-642.

80. **Grieve AG, Rabouille C.** 2011. Golgi bypass: skirting around the heart of classical secretion. Cold Spring Harb Perspect Biol **3**.

81. **Chwetzoff S, Trugnan G.** 2006. Rotavirus assembly: an alternative model that utilizes an atypical trafficking pathway. Curr Top Microbiol Immunol **309:**245-261.

FIGURE LEGENDS

Figure 1: Construction of E1-mCherry-labeled HCV Jc1 variants. (A) Schematic representation of HCV-Jc1 genomes generated in this study. Depicted above is for reference the HCV-Jc1 genome. Based on this we modified the backbone to express mCherry within the E1 glycoprotein with or without NS5A-GFP, Flag-E2 or the A4 epitope in E1 for recognition by the anti-E1 A4 antibody (see Material and Methods for details). Green box, GFP; red box, mCherry; blue box, Flag tag. **(B)** 48 hours post electroporation (hpe) with RNA of Jc1-WT, Jc1-ΔE1/E2 or variants of the Jc1-E1(A4) Huh7.5 cells were lysed and expression of viral proteins was analyzed by Western blotting. Shown are representative blots of at least three individual experiments. **(C)** Confocal images of HCV-Jc1-E1(A4) and HCV-Jc1-E1(A4)-mCherry electroporated Huh7.5 at 48 hpe cells show subcellular localization of viral proteins visualized by immunofluorescence staining and localization of E1-mCherry. Scale bar: 35 µm.

Figure 2: Characteristics of Jc1-E1(A4)-mCherry variants. (A) Huh7.5 cells were electroporated with RNA of Jc1-E1(A4), Jc1-E1(A4)/NS5A-GFP, Jc1-E1(A4)-mCherry, or Jc1-E1(A4)-mCherry/NS5A-GFP and harvested at the indicated time points to be fixed, permeabilized and stained for HCV Core before analysis by flow cytometry. Shown is the percentage of Core positive cells over a time course of 64 hpe. Error bars indicate standard

deviation (SD) of two individual biological replicates per data point. **(B)** Huh7.5 cells were electroporated with RNA of the indicated viruses. Supernatants were collected 65 hpe, cleared by centrifugation and filtration and concentrated by ultracentrifugation before they were used for infection of naïve Huh7.5 cells. Infected cells were harvested 72 hpi, stained for expression of intracellular Core in the case of mock and Jc1-E1(A4) infected cells and MFI was analyzed by flow cytometry. The percentage of infected cells was calculated relative to the number of Core-positive cells electroporated with the indicated RNAs and then normalized to Jc1-E1(A4)-infected cells; n.s., no signal.; FACS plots are shown to illustrate the shift of cells when they express the corresponding fluorescent viral proteins. **(C)** Shown is the mean fluorescence intensity (MFI) of the HCV Core positive cell population from A over a time course of 64 hpe. **(D)** Huh7.5 cells electroporated with RNA of HCV Jc1-E1(A4) or HCV Jc1-E1(A4)-mCherry/NS5A-GFP were lysed at the indicated time points and expression of viral proteins was analyzed by Western blotting. Actin was used as a loading control. Shown are representative blots of two individual experiments. **(E)** Intracellular RNA and **(F)** RNA from supernatants of Huh7.5 cells electroporated with the indicated HCV RNAs (comp. panel A) were extracted, and qRT-PCR was performed as described in the material and methods section to quantify the amount of vRNA genomes. The number of genomes was normalized to the percentage of HCV expressing cells as assessed by Core staining (comp. A). Error bars indicate SD of two individual biological replicates per data point. **(G)** Huh7.5 cells were electroporated with RNA of Jc1-E1(A4), Jc1-E1(A4)/Flag-E2, or Jc1-E1(A4)-mCherry/Flag-E2 and lysed 48 hpe. Lysates were subjected to immunoprecipitation (IP) using an antibody against Flag and blotted against Core, E1(A4) and E2. Shown are representative blots of three individual experiments. **(H)** Huh7.5 cells were electroporated with RNA of Jc1-E1(A4) or Jc1-E1(A4)-mCherry and supernatants

harvested 72 hpe were subjected to ultracentrifugation and density gradient fractionation. Proteins of the different fractions were separated by SDS-PAGE and analyzed by Western blotting. Shown are representative blots of three individual experiments (one of the latter including detection of ApoE, sell lower panel). **(I)** Aliquots of the fractions obtained in (E) were used for RNA extraction and subsequent qRT-PCR analysis to detect vRNA genomes. Error bars indicate SD of three individual experiments.

Figure 3: Tempo-spatial formation of NS5A-GFP replication complexes and E1(A4)-mCherry punctae. Huh7.5 cells were electroporated with RNA of Jc1-E1(A4)-mCherry/NS5A-GFP. **(A)** A confocal image of living cells showing mCherry and GFP fluorescence was taken every 24 h for up to 96 hpe (see also Supplemental Movies S1-S6). Shown are representative images from two individual experiments with 22 and 38 analyzed cells, respectively. Scale bars: 9 µm. White boxes indicate areas of magnification. **(B)** Cells imaged as described were analyzed for punctae of E1(A4)-mCherry and NS5A-GFP with an arbitrarily chosen maximum threshold of 0.8 µm diameter. Punctae were counted with the spot counting tool (Volocity). Each dot indicates the number of punctae in one cell, whereby red dots represent E1(A4)-mCherry punctae and green dots represent NS5A-GFP punctae. **(C)** Ratios of E1(A4)-mCherry accumulation to NS5A-GFP accumulations were calculated for each cell. Differences in (B) and (C) were assessed for statistical significance with a one-way ANOVA with post test; *, $p \leq 0.05$; **, $p \leq 0.01$; ***, $p \leq 0.001$; ns, not significant.

Figure 4: Temporal dynamics of viral protein interactions at E1(A4)-mCherry punctae. Huh7.5 cells were electroporated with RNA of Jc1-E1(A4)-mCherry and fixed at the indicated time points and processed for proximity ligation assay (PLA) with primary antibodies against mCherry and either E2, or Core, or NS3, or NS5A depending on the interaction analyzed. **(A)**

971 Representative magnified and cropped images to show areas of PLA positive samples stained for
972 E1(A4)-mCherry and E2 or E1(A4)-mCherry and Core at 48 hpe and 72 hpe. White arrows show
973 exemplary E1(A4)-mCherry punctae with a positive PLA signal. Scale bar: 3.5 µm. **(B)**
974 Quantitative analysis of PLA positive punctae/cell is shown for ≥ 20 cells per condition using the
975 spot counting tool (Volocity) with an arbitrarily chosen maximum threshold of 0.8 µm.
976 Differences were assessed for statistical significance with a one-way ANOVA with post test; *,
977 $p \leq 0.05$; **, $p \leq 0.01$; ***, $p \leq 0.001$; ns, not significant.
978
979 **Figure 5: E1(A4)-mCherry punctae do not colocalize with Golgi but ER and endosomal**
980 **markers. (A)** Living Huh7.5 cells coelectroporated with RNA of Jc1-E1(A4)-mCherry and
981 plasmids expressing GalT-CFP, ApoE-GFP or CD74(Ii)-CFP **(B)** or Huh7.5 coelectrporated with
982 plasmids encoding for GalT-CFP and HBV-S-mCherry or Gaussia-YFP were analyzed by
983 confocal microscopy 56 hpe. Images were merged and colocalization was analyzed by a
984 fluorescence line profile and **(C)** by calculation of the Pearsons R^2 value. The number of cells
985 analysed is indicated above every column. Differences were assessed for statistical significance
986 with a one-way ANOVA with post test; ns, not significant; ****, $p \leq 0.0001$. Scale bar: 11µm.
987 The white square depicts the area that was digitally magnified. The fluorescence intensity in the
988 line profiles is given in arbitrary fluorescence units (AU).
989
990 **Figure 6: Glycoproteins on released HCV particles are EndoH sensitive.** Huh7.5 cells were
991 transfected with a plasmid encoding HBV-S **(A)** or electroporated with RNA of Jc1-E1(A4) **(B-**
992 **D)**. **(A)** Western blot of supernatants from HBV-S expressing cells at 72 hours post transfection
993 that were concentrated by ultracentrifugation and treated with EndoH (0.5 µl) and PNGaseF (0.1

µl) as indicated. **(B)** Lysates from Jc1-E1(A4) electroportated Huh7.5 cells were generated at 72 hpe and digested with 0.5 µl EndoH and PNGaseF or (**C)** increasing doses of EndoH (0 µl, 0.01 µl**,** 0.05 µl and 0.5 µl) or PNGaseF (0 µl, 0.01 µl**,** 0.025 µl and 0.1 µl) to assess dose dependency by Western blotting. **(D)** Supernatant from Jc1-E1(A4) electroportated Huh7.5 cells was collected at 72 hpe, concentrated and density gradient fractionated as described in Materials and Methods. The individual fractions were digested with 0.5 µl EndoH and 0.1 µl PNGaseF before Western blot. The density of the fractions depicted were 1.06g/ml (3), 1.08g/ml (4), 1.12g/ml (5) and 1.16g/ml (6). We show one representative experiment of at least three independent biological replicates.

Figure 7: E1(A4)-mCherry punctae traffic with Rab9A positive compartments. (A) Living Huh7.5 cells coelectroporated with RNA of Jc1-E1(A4)-mCherry and plasmids encoding VSV-G-GFP, Rab7A-CFP, and Rab9A-CFP were analyzed using by confocal microscopy 48 hpe. Scale bars: 11 µm. The fluorescence intensity in the line profiles is given in arbitrary fluorescence units (AU). Green lines represent GFP/CFP fluorescence, red lines represent E1(A4)-mCherry fluorescence. **(B)** Living Huh7.5 cells coelectroporated with RNA of Jc1-E1(A4)-mCherry and a plasmid encoding Rab9A-CFP were used for fluorescence recovery after photobleaching (FRAP) analysis 53 hpe. Scale bar: 11µm. White circles indicate areas that were photobleached (1 and 2) and fluorescence recovery was imaged over a time period of 288 s (compare Supplemental Movie S8). Representative images of indicated time points are shown. **(C)** Fluorescence intensity profile of the depicted areas was assessed over time and normalized relative to the fluorescence intensity in the bleached area before FRAP (set as 100 %). The black line represents fluorescence recovery of circle 1, the dark grey line of circle 2. Multiple cells and

1017 punctae with E1(A4)-mCherry and/or Rab9A-CFP fluorescence were analyzed with FRAP and
1018 results were similar to the representative sequence shown here (also compare Supplemental
1019 Movie S8).
1020
1021 **Figure 8: HCV but not Gaussia luciferase release is suppressed by inhibition of the**
1022 **endosomal compartment. (A)** Huh7.5 cells were electroporated with HCV Jc1-luc RNA. 40
1023 hpe medium was changed and fresh medium containing the indicated drugs was added.
1024 Additional eight hours later supernatants were harvested and sucrose gradient centrifuged in
1025 order to remove the drugs and purify newly produced virus. Pellets were resuspended and used to
1026 inoculate uninfected Huh7.5 cells. 72 hours later cells were lysed and luciferase activity, hence
1027 viral infection, was quantified. The graph shows mean values and standard error of the mean
1028 (SEM) from four to nine independent electroporation. In the lower panel we measured Jc1-luc
1029 activity in lysates of the producer cells. (B) Same experimental setting as in (A), however
1030 Huh7.5 cells were electroporated with a Gaussia luciferase reporter construct. Eight hours later
1031 supernatants were taken and secreted Gaussia luciferase was quantified. The graph shows mean
1032 values and SEM from six independent electroporations. (C) Huh7.5 cells were electroporated
1033 with HCV JC1-luc RNA. 40 hpe cells were starved and either transferrin (Tf) or transferrin
1034 conjugated with Horseraddish peroxidase (HRP-Tf) was added and allowed to internalize for two
1035 hours. Subsequently, endosomes were chemically fixed inside living cells as described in the
1036 method section and before (44, 45). Next, medium was changed and cells were allowed to
1037 produce virus for additional eight hours. Supernatants were taken, sucrose gradient purified and
1038 used to inoculate uninfected Huh7.5 cells in order to quantify the amount of released virus.
1039 Furthermore Jc1-luc activity was quantified by measurement of luciferase activity in the

producer cells (lower panel). Depicted are mean values and SEM from 15 independent electroporations. (D) Same experimental design as in (C) except that a Gaussia luciferase reporter construct was electroporated. Furthermore the amount of released Gaussia luc was directly quantified in the supernatants. Shown are mean values and SEM from seven independent experiments. Differences were assessed for statistical significance with a one-way ANOVA with post test ; **, $p \leq 0.01$; ****, $p \leq 0.0001$.

Figure 1

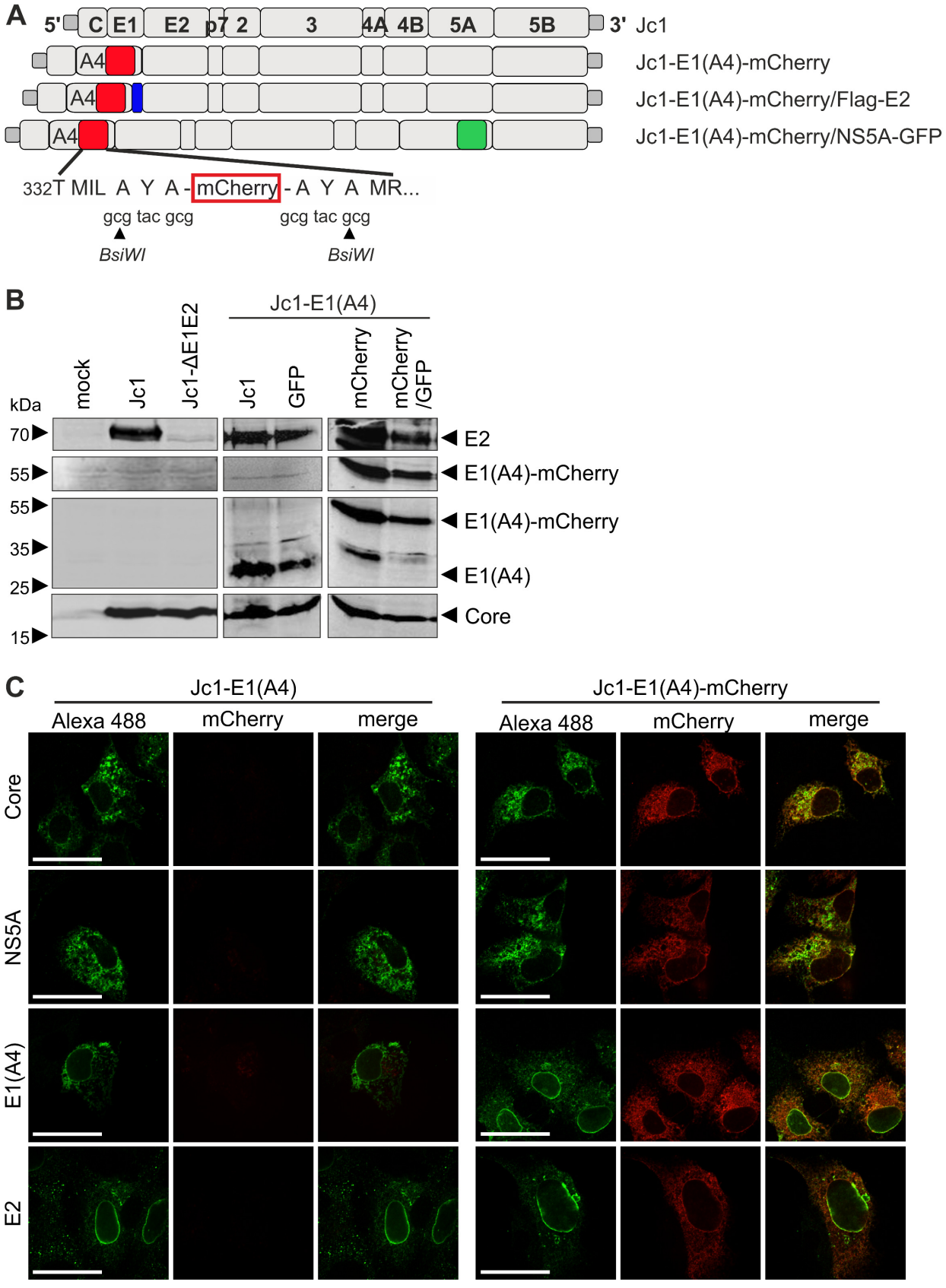

Figure 2

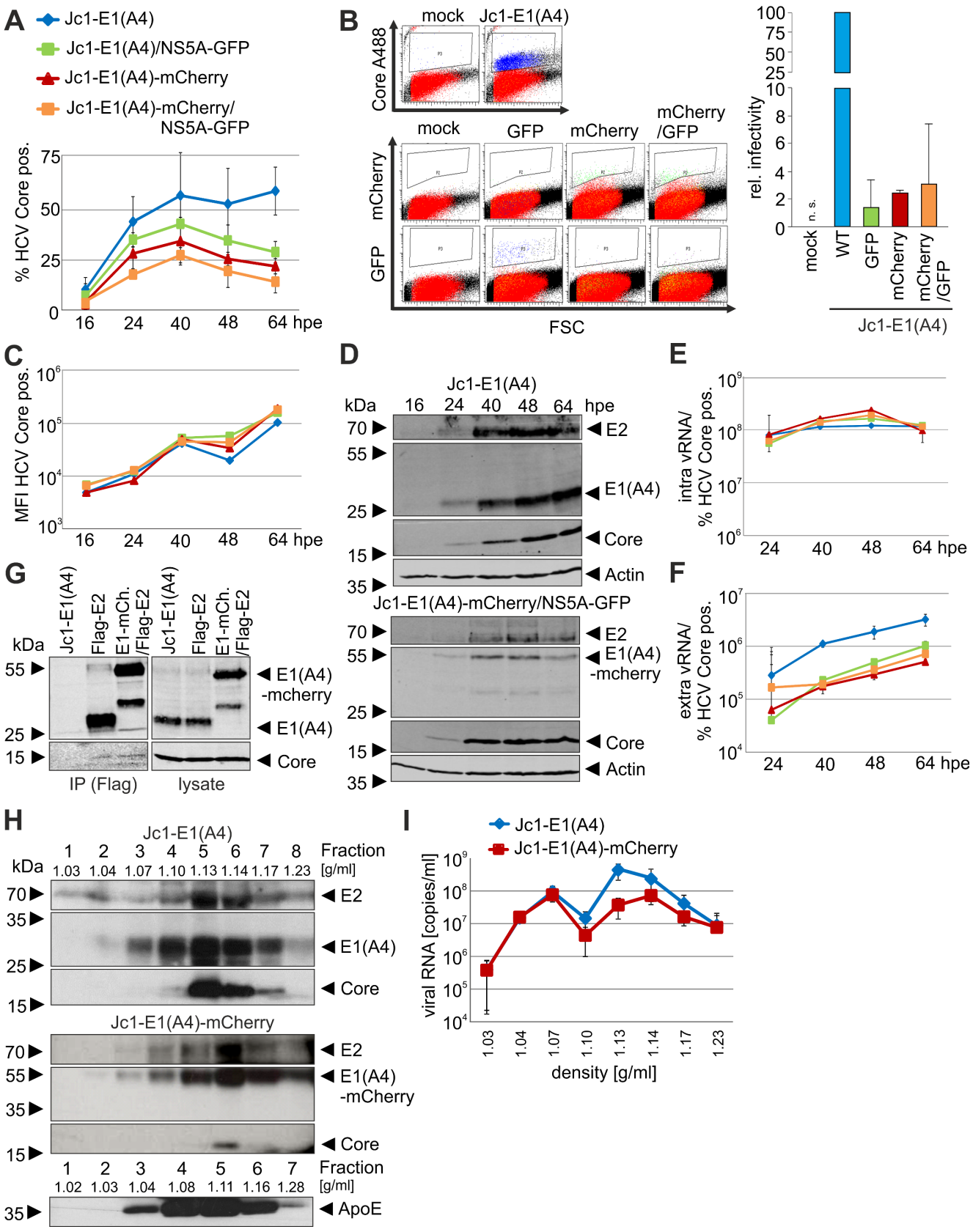

Figure 3

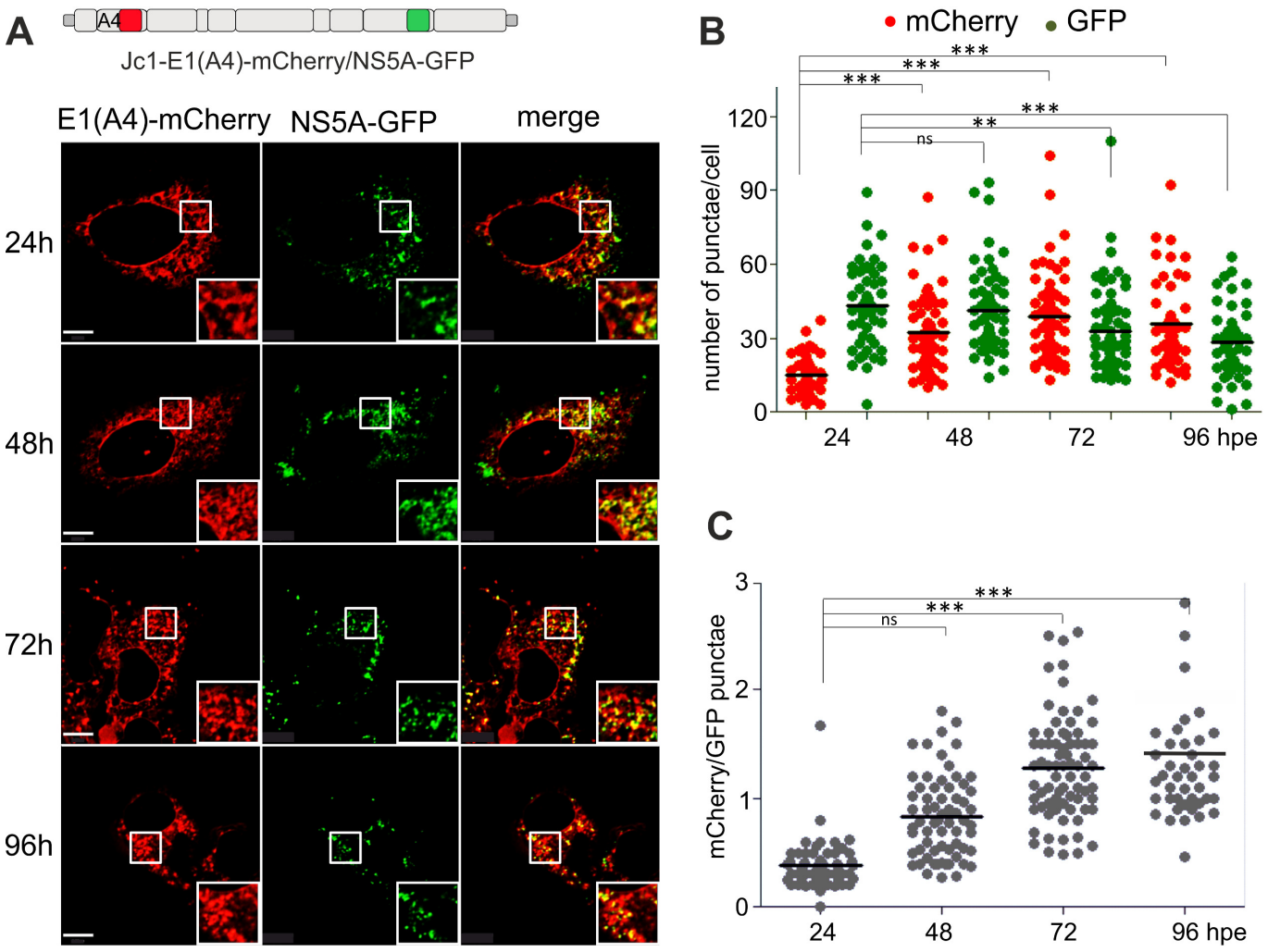

Figure 4

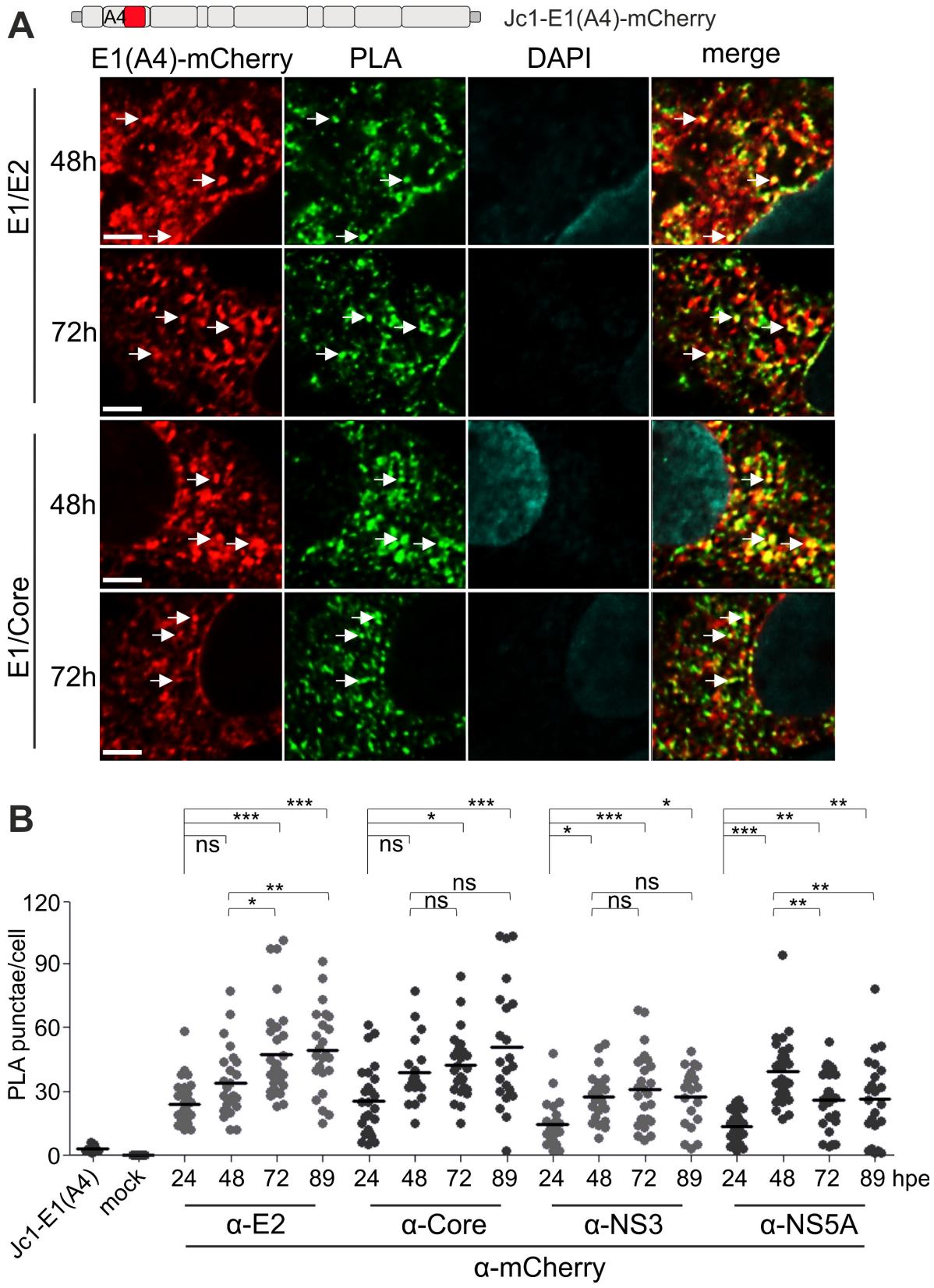

Figure 5

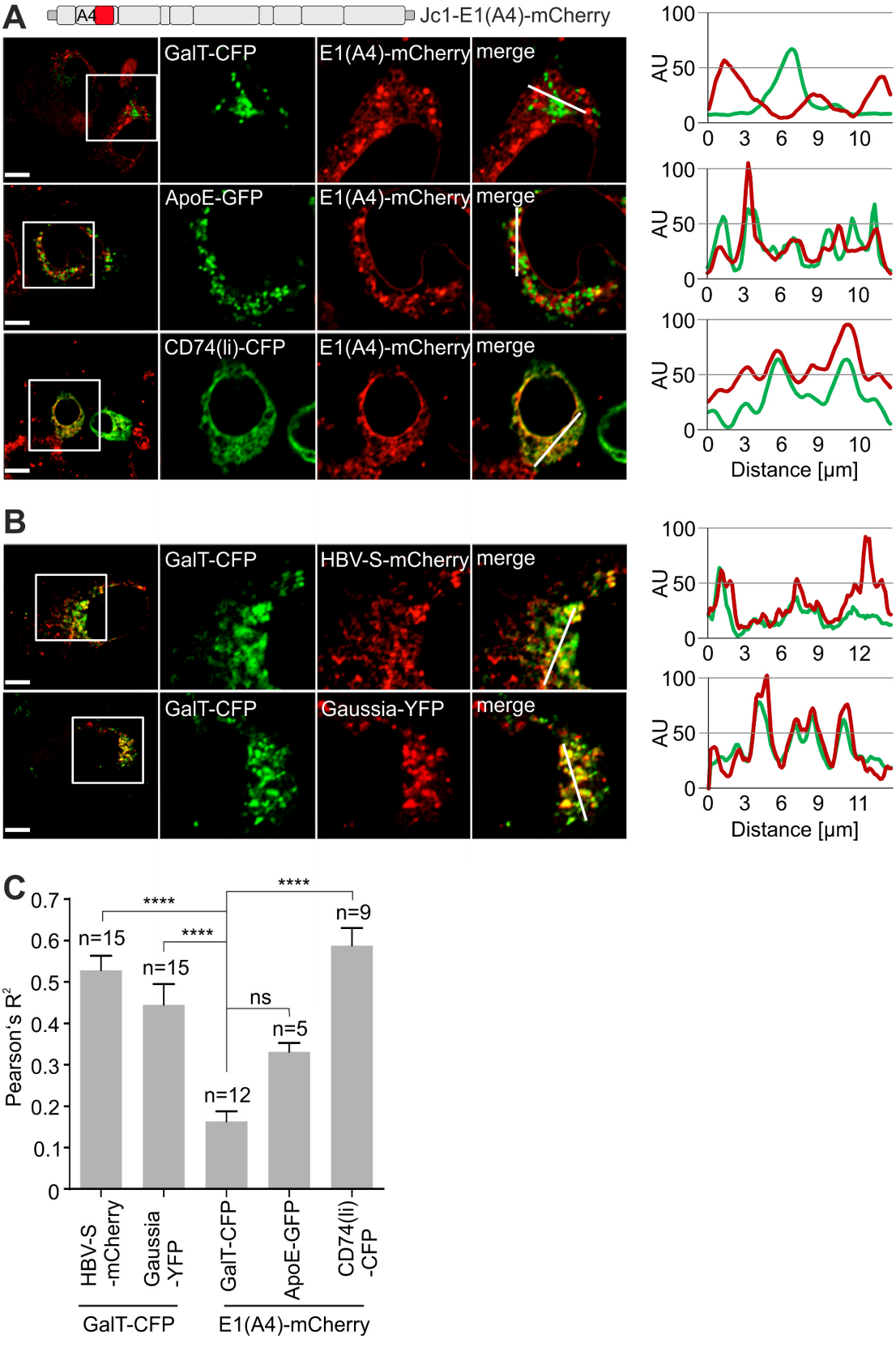

Figure 6

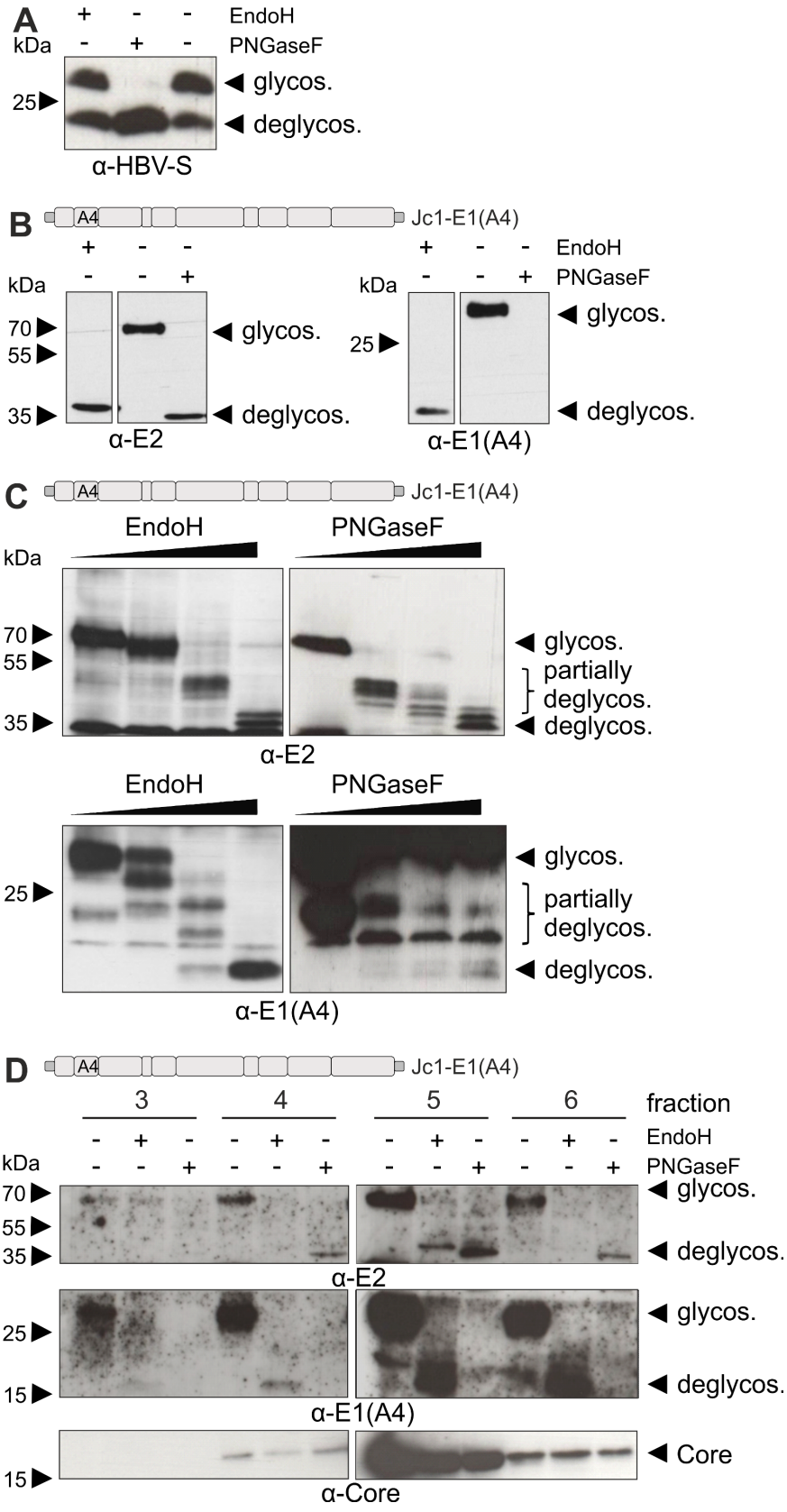

Figure 7

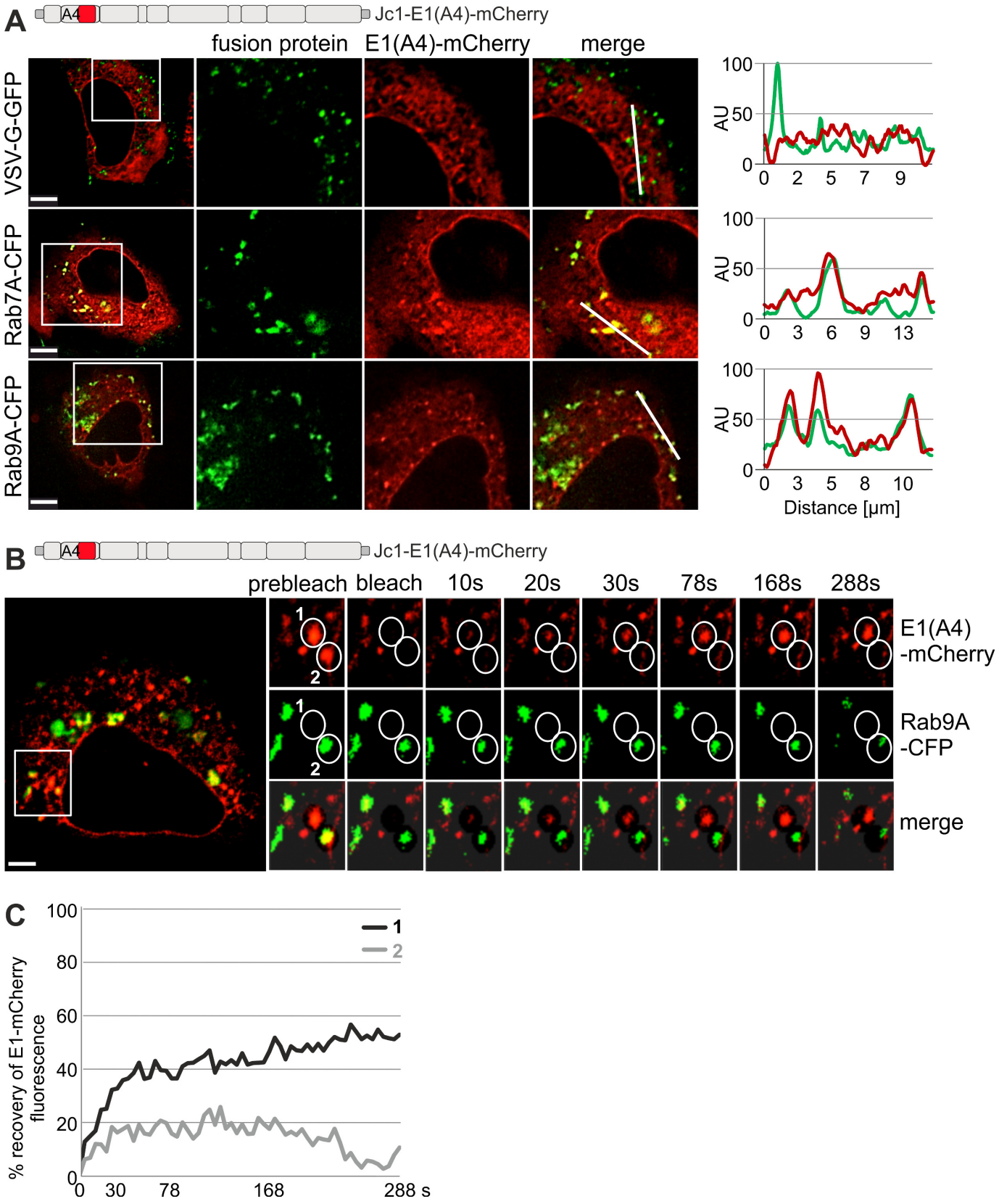

Figure 8